ANL/CEN/FE-78-4

ANL/CEN/FE-78-4

SUPPORT STUDIES IN FLUIDIZED-BED COMBUSTION

Quarterly Report
April—June 1978

by

Irving Johnson, G. J. Vogel, S. H. D. Lee, J. A. Shearer, R. B. Snyder, G. W. Smith, E. B. Smyk, W. M. Swift, F. G. Teats, C. B. Turner, W. Ira Wilson, and A. A. Jonke

ARGONNE NATIONAL LABORATORY, ARGONNE, ILLINOIS

Prepared for the U. S. DEPARTMENT OF ENERGY
under Contract W-31-109-Eng-38

DISCLAIMER

Printed in the United States of America
Available from
National Technical Information Service
U. S. Department of Commerce
5285 Port Royal Road
Springfield, Virginia 22161
Price: Printed Copy $6.00; Microfiche $3.00

Distribution Category:
Coal Conversion and Utilization—
Direct Combustion of Coal
(UC-90e)

ANL/CEN/FE-78-4

ARGONNE NATIONAL LABORATORY
9700 South Cass Avenue
Argonne, Illinois 60439

SUPPORT STUDIES IN FLUIDIZED-BED COMBUSTION

Quarterly Report
April—June 1978

by

Irving Johnson, G. J. Vogel, S. H. D. Lee, J. A. Shearer,
R. B. Snyder, G. W. Smith, E. B. Smyk, W. M. Swift,
F. G. Teats, C. B. Turner, W. Ira Wilson,
and A. A. Jonke

Chemical Engineering Division

Prepared for the
U. S. Department of Energy
under Contract No. W-31-109-Eng-38
and the
U. S. Environmental Protection Agency
under Agreement IAG-D5-E681

Previous reports in this series

ANL/CEN/FE-77-8
ANL/CEN-FE-77-11
ANL/CEN/FE-78-3

BIBLIOGRAPHIC DATA SHEET	1. Report No. ANL/CEN/FE-78-4	2.	3. Recipient's Accession No.
4. Title and Subtitle Support Studies in Fluidized-Bed Combustion, Quarterly Report, April—June 1978			5. Report Date July 1978 6.
7. Author(s) I. Johnson, G. J. Vogel, S.H.D. Lee, J. Shearer, R. Snyder, G. Smith, W. Swift, F. G. Teats, C. Turner, I. Wilson & A. A. Jonke			8. Performing Organization Rept. No. ANL/CEN/FE-78-4
9. Performing Organization Name and Address Argonne National Laboratory 9700 South Cass Avenue Argonne, Illinois 60439			10. Project/Task/Work Unit No. 11. Contract/Grant No. W31-109-Eng-38 (DOE) IAG-D5-E681 (EPA)
12. Sponsoring Organization Name and Address U. S. Department of Energy and the U. S. Environmental Protection Agency			13. Type of Report & Period Covered April-June 1978 14.

15. Supplementary Notes

16. Abstracts This work supports the development studies for atmospheric and pressurized fluidized-bed coal combustion. Laboratory and process development studies are aimed at providing needed information on limestone utilization, control of emission of alkali metal compounds and SO_2 during combustion, particulate loadings of flue gas, and other aspects of fluidized-bed coal combustion. This report presents information on: the SO_2 reactivities and thus the limestone requirements of sixty different limestones, the morphology of a few selected stones, the effect of water in the gaseous mixture on the SO_2 reactivities of three limestones, the effect of combustion conditions on the attrition of limestones, the effect of temperature on SO_2 retention by limestone in a carbon burnup cell, the effect of $CaCl_2$ and $MgCl_2$ additives on the SO_2 capacity of limestones, the use of diatomaceous earth and activated bauxite to remove alkali metal compounds from simulated combustion gas mixtures, selection of laser spectroscopy methods to be evaluated for the measurement of gaseous alkali metal species in hot flue gases, the application of acoustic dust conditioning to flue gas cleaning, and the conceptual design of a granular-bed filter for cleaning of flue gas in a 200-MWe fluidized-bed combustion facility.

17. Key Words and Document Analysis. 17a. Descriptors

Abrasion
Additives
Air Pollution
Calcium Chloride
Calcium Oxides
Calcium Sulfates
Coal
Combustion
Corrosion
Cyclone Separators
Diatomaceous Earth
Dolomite
Flue Gas
Fluidized Bed Combustion
Fossil Fuels
Limestone
Magnesium Chlorides
Porosity
Roasting
Sodium Chlorides
Sulfur Oxides

17b. Identifiers/Open-Ended Terms

Acoustic Dust Conditioning
Activated Bauxite
Alkali Metal Sulfates
Carbon Burnup Cell
Granular Bed Filter
Laser Spectroscopy
Limestone Compositions
Sorbent Regeneration
Sorbent Sulfation
Stone Morphology
Sulfate Corrosion

17c. COSATI Field/Group 13B

18. Availability Statement	19. Security Class (This Report) UNCLASSIFIED	21. No. of Pages
	20. Security Class (This Page) UNCLASSIFIED	22. Price

TABLE OF CONTENTS

TABLE OF CONTENTS (contd)

LIST OF FIGURES

LIST OF TABLES

SUPPORT STUDIES IN FLUIDIZED-BED COMBUSTION
QUARTERLY REPORT

April—June 1978

by

Irving Johnson, G. J. Vogel, S. H. D. Lee, J. A. Shearer,
R. B. Snyder, G. W. Smith, E. B. Smyk, W. M. Swift,
F. G. Teats, C. B. Turner, W. Ira Wilson,
and A. A. Jonke

ABSTRACT

This work supports the development studies for atmospheric and pressurized fluidized-bed coal combustion. Laboratory and process development studies are aimed at providing needed information on limestone utilization, control of emission of alkali metal compounds and SO_2 during combustion, particulate loadings of flue gas, and other aspects of fluidized-bed coal combustion.

This report presents information on: the SO_2 reactivities and thus the limestone requirements of sixty different limestones, the morphology of a few selected stones, the effect of water in the gaseous mixture on the SO_2 reactivities of three limestones, the effect of combustion conditions on the attrition of limestones, the effect of temperature on SO_2 retention by limestone in a carbon burnup cell, the effect of $CaCl_2$ and $MgCl_2$ additives on the SO_2 capacity of limestones, the use of diatomaceous earth and activated bauxite to remove alkali metal compounds from simulated combustion gas mixtures, selection of laser spectroscopy methods to be evaluated for the measurement of gaseous alkali metal species in hot flue gases, the application of acoustic dust conditioning to flue gas cleaning, and the conceptual design of a granular-bed filter for cleaning of flue gas in a 200-MWe fluidized-bed combustion facility.

SUMMARY

Task A. Gaseous Pollutant Emission Control in Fluidized-Bed Combustion (FBC)

Included in this task is work on SO_2 emission control, limestone characterization, and chemical enhancement of limestone reactivity.

Reactivity of Limestones with Sulfur Dioxide. The SO_2 reactivities of 60 different limestones have been measured, using a thermal gravimetric analyzer and the results were used to predict the performance of the stones in an atmospheric fluidized-bed combustor. Estimates were made for combustor superficial gas velocities of 2.4 and 3.6 m/s and for retentions of 83 and 90% of the sulfur dioxide liberated by the combustion of a coal containing

4.3% sulfur. At a gas velocity of 2.4 m/s, about one-half of the stones tested are predicted to require 0.5 kg or less of stone per kg of coal in order to meet the 83% sulfur retention requirement, and 1 kg or less of stone per kg of coal is required to meet the 90% sulfur retention requirement. At a superficial gas velocity of 3.6 m/s, about one-third of the stones required 1 kg or less of stone per kg of coal to meet the 90% retention requirement.

Petrographic Examination of Limestones. As the preceding section indicates, there is a wide variation in the SO_2 reactivity of limestones having essentially the same chemical composition. In an attempt to understand the causes of these differences, the morphologies of a few selected stones have been determined, using petrographic methods. Two calcitic and two dolomitic limestones representative of low and high SO_2 reactivity were examined. The highly reactive dolomite was made up of small grains and was highly porous while the poorly reactive dolomite contained very coarse grains. The highly reactive calcitic limestone contained very small grains and had high porosity while the poorly reactive stone consisted of fine grains but had very low porosity. A stone which is a "popper" (*i.e.*, explodes on calcination) was examined. The grains of this stone contained a large number of submicroscopic inclusions which may be related to its tendency to decrepitate when calcined.

Effect of Water on SO_2 Reactivity. The SO_2 reactivity of three limestones was measured in a TGA with gaseous water (~7%) present and absent from the sulfation gas mixture. The extent of conversion of the $CaCO_3$ to $CaSO_4$ was the same, whether gaseous water was present or absent.

Attrition of Limestone. To evaluate the potential utility of a limestone its rate of attrition under FBC conditions must be considered. To determine the influence of calcination, sulfation, and temperature on the rate of attrition, laboratory studies have been done using two different limestones and one dolomite (-14 +30 mesh). The higher temperature (870 *vs.* 25°C) had differing effects on the attrition rates of the limestones (2203 and Greer) and dolomite (Tymochtee). The attrition rate at 870°C for all three stones was not significantly changed by precalcination. Tests made under simultaneous calcination-sulfation conditions at 870°C indicated that the rate of attrition was either unchanged or decreased from the rate measured under calcination conditions.

Carbon Burnup Cell Studies. A process development unit (PDU) has been operated between 850 and 1100°C with various limestone bed materials. The results suggest that SO_2 retention is a strong inverse function of temperature. At 1100°C, essentially no SO_2 was retained by virgin or by previously sulfated limestones or dolomites.

Enhancement of Limestone Sulfation. Enhancement of the SO_2 capacity of limestones by the use of additives (small amounts of various alkali metal or alkaline earth salts) is being studied. Such enhancement could result in a significant decrease in the amount of limestone needed for the control of SO_2 emissions from FBC systems. Calcium chloride is being evaluated as an additive. Tests on fifteen different limestones indicate that a lower concentration of $CaCl_2$ than of NaCl is needed to achieve optimum SO_2 reactivity enhancement. It was found that small additions of $CaCl_2$ affect the SO_2 reactivity of limestone by the same mechanism as for NaCl (studied earlier), *i.e.*, by increasing the average pore diameter of the stone particles.

Pore diameters for maximum conversion of CaO to $CaSO_4$ range from 0.2 to 0.4 μm.

The effect of $MgCl_2$ on the SO_2 reactivity of four representative stones was studied; $MgCl_2$ behaved nearly the same as $CaCl_2$.

Pore volume-pore diameter profiles have been compared for four different stones, using NaCl, $CaCl_2$, and $MgCl_2$ each at the 0.5 mol % level. The largest increases in average pore diameter from adding these salts were produced in the purest stones and the smallest increases in the stones having the highest impurity levels. Other data give the SO_2 reactivity for four different stones and, in turn, each of the additives, NaCl, NaOH, Na_2CO_3, Na_2SO_4, Na_2SiO_3, $Na_2SiO_3 \cdot 9H_2O$, $CaCl_2$, $MgCl_2$, $Ca(OH)_2$, $CaSO_4$, and H_3BO_3 at a concentration of 1 mol %.

Task B. Turbine Corrodent Studies

Included in this task is work on the emission of alkali metal compounds from combustion systems and on methods for the removal from hot flue gases of alkali compounds (rather than all particulates reported in Task D). Results are reported on studies of the use of granular sorbents for the removal from a hot gas stream of gaseous alkali metal chlorides and the preliminary results of an evaluation of laser spectroscopy systems (Appendix C) potentially useful for *in situ* gaseous species measurement on hot flue gases.

Removal of Alkali Metal Compounds from Hot Flue Gas of Coal Combustion.

Solid sorbents are under study for the removal of gaseous alkali metal compounds from hot flue gases. A laboratory-scale horizontal combustor vessel is used. Resistance heating is used to heat the fixed bed of sorbent and induction heating to vaporize the alkali metal compound. Diatomaceous earth and activated bauxite were earlier found to be effective materials for the removal of gaseous NaCl and KCl from simulated combustion gas mixtures. The effects of temperature (in the range 800-880°C) and the duration of tests (1 to 6 h) have been studied for these two sorbents. The capacity of the diatomaceous earth was greater than that of the activated bauxite on a weight basis but was less than that of activated bauxite on a volume basis. It was found the sorption capacity of both sorbents increases nonlinearly with experimental time. This suggests that under the experimental conditions, the reaction rate between NaCl and diatomaceous earth and the adsorption of NaCl on activated bauxite are not controlled by the mass transfer of NaCl vapor from the bulk of flue gas to the external surface of the sorbent.

Development and Application of a Laser Spectroscopy System for FBC Gas Species Measurement (Reported in Appendix C). The use of a laser spectroscopy system for the quantitative measurement of gaseous alkali metal species in hot flue gases is under investigation. A preliminary evaluation has been made of most possible methods, and three have been chosen for more detailed study: (1) resonant absorption near 9 μm, (2) intense local heating to yield ionized sodium, and (3) photolytic dissociation of sodium chloride.

Task D. Particulate Control Studies

An experimental program is continuing at ANL to test and evaluate promising flue gas cleaning methods in the flue gas system of the 15.2-cm-dia-PFBC. Techniques being investigated are acoustic dust conditioning, high efficiency controlled-vortex cyclones, and granular-bed filters.*

Acoustic Dust Conditioning. Work is currently being carried out at the University of Toronto under a subcontract to develop and fabricate a pulse-jet sound generator, a resonant manifold, and acoustic treatment sections for subsequent installation and testing in the flue gas system of the ANL combustor.

Prototype pulse-jets are currently being fabricated and tested at ambient conditions to finalize the design of the pulse-jet for operation at elevated pressure. Typical qualitative capabilities are a sound intensity of 135 dB at 200 to 450 Hz.

Fabrication of the resonant manifold has also been completed. Initial testing at ambient pressure is scheduled to begin shortly.

The instrumentation arrangements for pressure and flow control between the pulse jet-resonant manifold system and the pressurized FBC have been developed.

TAN-JET Cyclone. A Donaldson Company high-efficiency controlled-vortex cyclone has been received for installation and testing in the ANL FBC system.

Granular-Bed Filter. Currently, a conceptual design of a granular-bed filter for a 200-MWe demonstration FBC facility is being made, based on experimental results previously reported. Presented are mass balances around the combustor and granular bed to assess the permissible working range of parameters for the granular bed, such as bed depth and gas velocity through the bed.

*The use of granular-bed filters to remove alkali metal compounds is being investigated in Task B.

TASK A. GASEOUS POLLUTANT EMISSION CONTROL IN FBC

1. Reactivity of Limestones with Sulfur Dioxide
(R. B. Snyder and W. Ira Wilson)

Sixty-one limestones* have been tested on the TGA for reactivity with SO_2 at 900°C using a gas mixture containing 0.3% SO_2 There is a large variability in the SO_2 reactivity of limestones and in the extent of conversion of the calcium carbonate to calcium sulfate. For the high-calcium (>90% $CaCO_3$) limestones tested, the conversion of $CaCO_3$ to $CaSO_4$ ranged from 19 to 66%; for the dolomites (40-60% $CaCO_3$), the range was 21 to 100%.

Using the limestone SO_2 reactivity curves (not shown), estimates were made of the quantity of limestone necessary per unit weight of coal to meet Federal SO_2 emission standards (Table 1). Estimates were made for a fluidized-bed coal combustor operated with a 0.9-m bed depth, superficial gas velocities of 2.4 m/s (8 ft/s) and 3.6 m/s (12 ft/s); the coal was assumed to contain 4.3% S with a heating value of 28,300 kJ/kg (12,200 Btu/lb). Estimates have been made for both the current SO_2 emission standard (1.2 lb $SO_2/10^6$ Btu, which for the coal considered requires 83% sulfur retention), and the new pending standard that requires 90% SO_2 retention. In Table 1, the kg of limestone/kg of coal required for the reactor operating with two different gas velocities and for the two SO_2 emission standards are given for 48 of the 62 stones tested.

For a reactor operated at 2.4 m/s (8 ft/s), 54% of the stones tested required less than 0.5 kg/kg of coal to meet the current standard and less than 1.0 kg/kg of coal to retain 90% of the sulfur. This included 38% of the dolomites (calcium carbonate percentage, 48 to 60%) and 65% of the limestones (percent calcium carbonate greater than 90%). For operation of a reactor at 3.6 m/s gas velocity, 13 of the 48 stones tested and analyzed (27%, *i.e.*, 27% of the dolomites and 25% of the limestones) required less than 1 kg/kg of coal to remove 90% of the sulfur. Eighty percent of all the stones could retain 90% of the sulfur with reactor operating at 3.6 m/s (12 ft/s). With a reactor operating at 2.4 m/s (8 ft/s), 98% of the stones could remove 90% of the sulfur.

These results suggest that a large fraction of the calcareous stones have a high reactivity with SO_2. Since limestones and dolomites are extremely plentiful throughout the United States, these results suggest that it would be highly likely that a stone having a high reactivity with SO_2 could be found near a chosen combustor site, minimizing limestone requirements and limestone disposal cost. Highly reactive stones (54% of the stones tested) would require between 0.25 and 0.5 kg of stone/kg of coal to meet the current SO_2 emission standard (with the combustor operating at 2.4 m/s). For 90% sulfur removal, 0.3-1.0 kg of these stones would be required per kilogram of coal.

It can be seen from Table 1 that increasing the sulfur retention requirement from 83% to 90% increases the limestone quantity, on the average, by ~90%

*The sources and compositions of the limestones used in these studies are given in Appendices A and B.

Table 1. Limestone Required to Meet Indicated EPA Standards, kg Stone/kg Coal

Limestone	Reactor A[a]		Reactor B[b]		TGA[c] Total Ca Utiliz., %	Quality of Stone[d]
	0.6 lb S/10^6 Btu	90% S Removal	0.6 lb S/10^6 Btu	90% S Removal		
ANL-4801	0.30	0.47	0.40	0.76	100.	**
ANL-4901	0.73	1.6	1.1	2.1	88.3	--
ANL-4902	0.30	0.56	0.43	1.3	96.2	*
ANL-4903	0.46	0.93	0.78	3.1	94.8	*
ANL-5001	--	--	--	--	--	--
Tymochtee (ANL-5101)	0.27	0.45	0.37	0.95	99.2	**
ANL-5102	0.60	1.1	0.86	2.6	91.3	--
ANL-5201	0.48	1.2	0.92	2.2	93.7	--
ANL-5202	0.46	1.1	0.82	2.1	94.8	--
ANL-5203	0.45	1.1	0.82	3.9	93.1	--
ANL-5204	0.74	1.3	1.0	3.9	56.8	--
ANL-5205	--	--	--	--	--	--
ANL-5206	0.39	0.52	0.45	0.70	100.	**
ANL-5207	1.2	5.8	2.4	Impossible	75.8	--
1337 (ANL-5301)	0.34	0.71	0.53	0.89	96.8	**
ANL-5302	0.98	2.5	2.0	Impossible	65.1	--
ANL-5303	0.83	1.5	1.3	3.3	68.9	--
ANL-5304	--	--	--	--	--	--
ANL-5401	--	--	--	--	97.7	--
ANL-5402	0.32	0.47	0.40	0.75	92.3	**
ANL-5403	--	--	--	--	97.2	--
ANL-5501	2.4	Impossible	Impossible	Impossible	21.3	--
Dolowhite (ANL-5601)	--	--	--	--	--	--
ANL-5602	0.89	1.3	1.2	2.5	44.8	--
ANL-5603	--	--	--	--	43.6	--
1351 (ANL-6101)	--	--	--	--	--	--

(contd)

Table 1. (contd)

Limestone	Reactor A[a] 0.6 lb S/10^6 Btu	Reactor A[a] 90% S Removal	Reactor B[b] 0.6 lb S/10^6 Btu	Reactor B[b] 90% S Removal	TGA[c] Total Ca Utiliz., %	Quality of Stone[d]
ANL-6301	0.37	0.62	0.49	1.2	79.7	*
ANL-6401	--	--	--	--	62.6	--
ANL-6501	0.49	1.4	0.93	Impossible	77.0	--
ANL-6701	0.28	0.46	0.37	0.95	81.3	**
ANL-6702	--	--	--	--	13.1	--
ANL-7401	0.62	1.2	0.79	2.5	65.8	--
Greer (ANL-8001)	0.48	0.89	0.73	2.2	53.2	*
1360 (ANL-8101)	0.47	0.57	0.51	0.88	53.6	**
ANL-8301	0.79	1.4	1.0	2.9	--	--
Chaney (ANL-8701)	0.30	0.39	0.34	0.66	60.8	**
1343 (ANL-8901)	--	--	--	--	--	--
ANL-8902	0.52	1.0	0.8	Impossible	44.0	--
ANL-8903	0.46	0.75	0.57	1.2	44.6	*
1335 (ANL-9201)	--	--	--	--	--	--
ANL-9401	0.35	0.50	0.44	0.89	52.5	**
ANL-9402	1.5	2.6	2.0	Impossible	26.5	--
Grove (ANL-9501)	0.56	0.69	0.62	1.3	37.5	*
ANL-9502	0.43	0.98	0.71	Impossible	55.6	*
ANL-9503	0.37	0.76	0.56	1.8	56.6	*
ANL-9504	0.44	0.61	0.51	1.1	43.9	*
ANL-9505	0.51	0.97	0.78	1.8	44.4	--
2203 (ANL-9601)	1.1	1.9	1.5	Impossible	32	--
ANL-9602	0.45	0.76	0.61	2.1	51.7	*

(contd)

Table 1. (contd)

Limestone	Reactor A[a] 0.6 lb S/10^6 Btu	Reactor A[a] 90% S Removal	Reactor B[b] 0.6 lb S/10^6 Btu	Reactor B[b] 90% S Removal	TGA[c] Total Ca Utiliz., %	Quality of Stone[d]
ANL-9603	0.55	0.81	0.68	0.97	32.1	*
Germany Valley (ANL-9701)	0.96	1.8	1.3	Impossible	18.7	--
ANL-9702	0.52	0.76	0.61	1.4	31.0	--
ANL-9703	0.27	0.32	0.28	0.42	66.2	**
ANL-9704	—	--	--	--	41.7	--
ANL-9705	0.41	0.78	0.57	1.8	46.2	*
ANL-9706	0.34	0.50	0.41	0.92	49.2	**
ANL-9801	0.52	0.81	0.67	1.4	35.3	--
ANL-9802	0.32	0.67	0.52	0.91	61.8	**
ANL-9803	—	--	--	--	--	--
ANL-9901	0.39	0.51	0.43	0.72	39.6	**
ANL-9902	0.31	0.81	0.51	Impossible	56.7	*
ANL-9903	0.51	0.98	0.80	1.9	45.9	--
Range	0.37-2.4	0.32-∞	0.28-∞	0.42-∞	--	--
Calcium-SO_2 Rate Constant, k	31.5	53.5	47	80	--	--

[a]Reactor A operates with a 0.9-m bed depth at 2.4 m/s.

[b]Reactor B operates with a 0.9-m bed depth at 3.6 m/s.

[c]This column lists the percentages of Ca in the limestone (-50 +70 mesh) that converts to $CaSO_4$ when the stone is first precalcined in 20% CO_2 at 900°C, then reacted at 900°C with a 0.3% SO_2-5% O_2-balance N_2 gas mixture for 3 h.

[d]One star is an arbitrary designation of a good limestone that requires less than 0.5 and 1.0 kg limestone/kg of coal when the EPA emission standards of 0.6 lb S/10^6 Btu input and 90% sulfur removal, respectively, must be met in Reactor A. Two stars is for a stone that not only meets the above requirements but also requires less than 1 kg/kg coal when Reactor B (12 ft/s) is used and 90% sulfur removal is required.

and ∿150% for a reactor operating at 2.4 m/s (8 ft/s) and 3.6 m/s (12 ft/s), respectively. The higher SO_2 retention (90%) requires a much larger calcium-SO_2 reactivity. From the fluid-bed desulfurization equation developed by Westinghouse,[1] the rate constant k for the calcium-SO_2 reaction can be calculated for the four sets of conditions studied. These reaction rate values (31.5, 53.5, 47, and 80) are given at the bottom of Table 1, where the rate constant has the unit, $^{-1}$. Notice that to increase the SO_2 retention from 83% to 90%, the reactivity or rate constant must be increased by ∿70%.

It should be noted that total calcium utilization determined with the TGA (Table 1) is not a good indicator of limestone performance in the combustor. For example, the conversions of $CaCO_3$ to $CaSO_4$ of ANL-5102, ANL-5201, and ANL-5203 are all above 90%; nevertheless, their limestone requirements are projected to be slightly higher than for the majority of the stones. As another example, if ANL-8001 (Greer) is compared with ANL-7401, ANL-7401 has a higher calcium conversion on the TGA, yet requires a greater amount of stone/kg of coal than does ANL-8001. A third example that illustrates the lack of correlation between calcium carbonate sulfation on a TGA and projected limestone requirements is a comparison of ANL-9901 and ANL-9902. For ANL-9902, 56.7% of the $CaCO_3$ is converted to $CaSO_4$, compared with 39.6% for ANL-9901. However, when 90% SO_2 retention is required, ANL-9901 requires less limestone than ANL-9902 does. Figure 1 shows the reactivity curves for the two stones. The sulfation of ANL-9901 is much faster than the sulfation of ANL-9902. Since the maximum SO_2 residence time in a fluid bed of 0.9-m bed depth with 3.6 m/s gas velocity is approximately 0.25 s, an important factor in obtaining high SO_2 retention is a high calcium-SO_2 reactivity. Thus, a desirable stone would have high reactivity along with a large total conversion of calcium to calcium sulfate. Thus, ANL-9901 is a superior stone to ANL-9902.

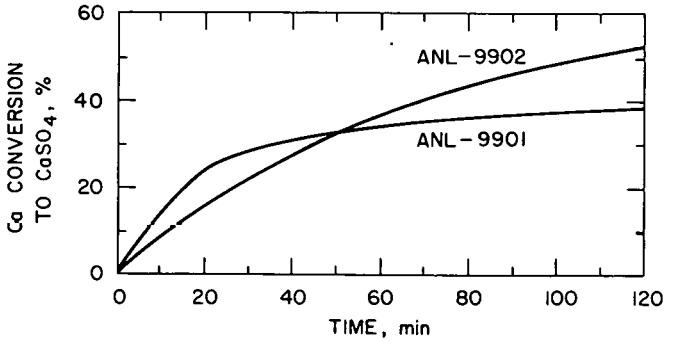

Fig. 1.

Reactivity Curves for ANL-9901 and ANL-9902 Stones.

The projections of limestone requirements given in Table 1 are sensitive to the rate of the calcium-SO_2 reaction--in other words, the slopes of the curves given in Fig. 1. Thus, small changes in rates of calcium conversion to $CaSO_4$ can produce large changes in projected limestone requirements. The results given in Table 1 are more reliable for comparisons of limestones than as absolute values. Finally, the purpose of giving the results in Table 1 to two significant figures is comparison of limestones with each other, not to suggest that the projected limestone requirements are accurate to two significant figures. The accuracy of the projected limestone requirements is not known, and they should be used with caution.

2. Petrographic Examination of Limestones

(R. B. Snyder, H. L. Fuchs,* and W. Ira Wilson)

The preceding section of this report indicates that there is a large variation in calcium utilzation for various limestones which have essentially the same chemical composition. It is believed that these differences in SO_2 capacity of stones of similar composition is due to variations in stone physical properties, such as porosity, grain size, and grain defects. To investigate this, five stones were selected for initial study (see Table 2). Two limestones were of similar composition but had widely different SO_2 reactivity. Two were dolomites having different SO_2 reactivities. The fifth one was chosen since it is a "popper"--that is, this stone explodes upon calcination. It is important to understand the latter property if the tendency of limestones to break up in fluidized beds is to be understood.

Petrographic examinations of the five calcareous rocks were performed by Fuchs.* His discussion of the results follows.

Polished sections were made of particulate samples from each of the five rocks following vacuum-impregnation with epoxy resin. These sections were examined in reflected polarized light. To find any inclusions which might affect the "popping" tendency during rapid temperature excursions, crushed particles were examined in transmitted light. Average grain sizes were estimated, and these may be in error by a factor of two. More reliable grain size measurements could be made by point counting several hundred grains in thin sections of each sample, but that method is more time-consuming than is the method chosen.

Table 2. Limestones Chosen for Study of Selected Physical Properties

Limestone	$CaCO_3$ Content, %	$MgCO_3$ Content, %	Conversion of Ca to $CaSO_4$ at 900°C in 3 h, %	Remarks
ANL-5402	54	27	92	--
ANL-5501	55	43	21	--
ANL-9802	98	0.5	62	--
Germany Valley	97	0.6	19	--
ANL-5001	50	43	--	This stone explodes upon calcination.

*Chemistry Division, Argonne National Laboratory.

a. ANL-5402 Dolomite

The ANL-5402 dolomite sample, more than any others, is heterogeneous in composition to the extent that the chemical analysis is not representative of any individual particle of the approximately 30 particles examined. White particles present are fine-grained calcite (micritic) with small amounts of dolomite barely detectable in the X-ray pattern. These make up about 15-20% of the sample. In contrast, most of the particles are grey porous dolomite containing small amounts of calcite. The average grain size of the dolomite is about 15 μm, but some particles are as large as 300 μm. Undoubtedly, the high porosity and high permeability of this sample contribute to its high reactivity. The 10% SiO_2 content indicated by the wet chemical analysis of the sample is not thought to be representative. Other examination indicated that the SiO_2 content is more likely to be 2-3%.

b. ANL-5501 Dolomite

This dolomite is analogous to marble, *i.e.*, it has been metamorphosed to a very coarse crystalline product. Grain sizes range from 0.2 to 1.0 mm, and the average grain size is between 0.5 to 0.7 mm. Inclusions of olivine, Mg_2SiO_4, are common and were probably formed by a reaction between the dolomite and country rock. Detrital olivines derived from basic igneous rocks contain a high concentration of fayalite (Fe_2SiO_4) component. Moreover, this dolomite contains some blue vesicular glass as veins, indicating a proximity to volcanic eruptions sometime in its history. The low reactivity of this stone probably results from its exceptionally large grain size produced by metamorphism.

c. ANL-9802 Limestone

It is difficult to estimate the average grain size from the polished section of this limestone because the finer grains tend to pluck out during polishing. Crushed particles viewed in transmitted light show that the average grain size is from 3 to 6 μm. Normally, the vacuum-impregnation treatment promotes greater retention of grains unless the permeability of those grains is low. The high reactivity of this limestone is probably linked with high porosity but limited somewhat by its apparently low permeability. The latter effect, however, may be negligible after calcination.

d. ANL-9701 (Germany Valley) Limestone

This limestone is fine-grained and dense for the most part but contains some coarser vein-deposited calcite. Grain sizes are predominantly in the 5 μm range. It is apparent that the fine-grained texture of this limestone is not conducive to high SO_2 reactivity. The densely packed crystallites have low porosity and low permeability. Impurities include small amounts of Fe_2O_3, quartz, and an undefined opaque phase which may be a sulfide other than FeS or FeS_2.

e. ANL-5001 Dolomite

This dolomite was studied as being a "popper". It is a coarse-grained equigranular rock displaying a recrystallization texture that is typical of most, if not all, coarse dolomites. Grain sizes range from 30 μm to 400 μm; the average size is ∿140 μm. The predominant impurities are chert

and quartz, and trace amounts of pyrite are present. Silica particles are often as large as the dolomite particles, and a sampling problem here could affect the measured SiO_2 content. Solution effects have opened some grain boundaries which are filled with noncalcareous cement. This feature could influence the integrity of some particles, increasing it or decreasing it, depending upon the nature of the cementing material.

The dolomite crystals are clouded with micron to submicron inclusions which appear opaque in transmitted light. The inclusions may be liquid, gaseous, or perhaps solid organics and their number might provide a rough indicator of "popping". ANL-5001 dolomite is very similar to ANL-5301 dolomite (1337). Both are coarse-grained and have clouded crystals, and it is uncertain why this stone is more of a "popper" than is 1337. The nature of inclusions, as well as their concentrations, may be significant.

f. Conclusion

There reamins some uncertainty as to whether the petrographic properties of the two fine-grained limestones (ANL-9802 and ANL9701) can account for their dfferences in reactivities. Porosity measurements may be better indicators of reactivity. It should be noted that although there may be some correlation between the petrographic properties of uncalcined calcareous rocks and their sulfation properties, the nature of their calcined products may be equally significant.

3. Effect of Water on SO_2 Reactivity
(R. B. Snyder and W. Ira Wilson)

The reactivity of limestones with SO_2 in the presence of oxygen has been investigated using a TGA. In these experiments, a synthetic combustion gas containing 0.3% SO_2, 5% O_2, and the balance N_2 has been reacted with the limestones. However, in a fluidized-bed combustor, the combustion gas contains approximately 7% H_2O. Therefore, three limestones were reacted with a mixture of 0.3% SO_2-5% O_2 gas containing various concentrations of H_2O. As can be seen in Table 3, the presence of H_2O in the reactant gas had essentially no effect on the limestone-SO_2 reactivity.

4. Limestone Attrition in a Fluidized Bed
(R. B. Snyder and W. Ira Wilson)

The attrition rate of two limestones and one dolomite have been studied. The attrition tests were performed in a 5.08-cm-ID quartz fluidized bed. A glass frit was used as the grid plate. The tube was heated by an external electrical furnace. The attrition tests were batch tests, with the starting materials each screened to -14 +30 mesh. The amount of attrition after 8-h tests was calculated by two different methods: (1) as the percentage of the original material that was lost overhead (all material lost overhead was smaller than 70 mesh) and (2) as the percentage of the original material smaller than 30 mesh. Four attrition tests were performed on each material: (1) precalcined material at 20°C in air, (2) precalcined material at 870°C in air, (3) the original material at 870°C in air, and (4) the original material at 870°C in 0.3% SO_2, the balance air. The difference in results for (1) and (2) was due only to the difference in operating temperatures. The effect of calcination on attrition rate can be found by comparing the results of (2)

Table 3. Reactivity of Various Limestones (-18 +20 mesh) at 900°C Using 0.3% SO_2-5% O_2-H_2O and N_2.

Limestone	H_2O in Synthetic Combustion Gas, %	Conversion of Ca to $CaSO_4$ in 2 1/2 h, %
ANL-9701[a]		
	0	12.0
	7	14.6
	25	12.8
	33.5	11.7
ANL-9501[b]		
	0	12.1
	7	12.4
ANL-8001[c]		
	0	37.7
	7	37.8

[a]Germany Valley limestone.

[b]Grove limestone.

[c]Greer limestone.

and (3). Finally, the effect of sulfation on stone attrition rate can be determined by comparing the results of tests (3) and (4). The results are given in Table 4 for Greer limestone, limestone 2203, and Tymochtee dolomite.

Several conclusions can be drawn from these results:

(1) The higher temperature (870°C) had differing effects on the attrition rates of the limestones (2203 and Greer) and dolomite. Additional experiments with dolomites are needed to determine the effect of temperature on attrition.

(2) Calcination has no effect on attrition rate. The attrition rates of precalcined and virgin material were identical for each stone. This conclusion is not valid for those limestones or dolomites that are "poppers".*

(3) Sulfation of stones generally decreases the attrition rate. Reductions in attrition due to sulfation for Tymochtee dolomite and limestone 2203 were 70% and 60%, respectively. Greer showed no attrition loss since this

*"Poppers" are stones which, as the particles rupture or break up upon calcination, make a popping sound. Some stones actually explode into very fine particles. Of the 65 stones tested to date, approximately 20% are "poppers".

Table 4. Limestone Attrition Tests

Test	Limestone (-14 +30 mesh)	Conditions	Wt % Loss After 8 h: Loss Overhead	Wt % Loss After 8 h: Material Smaller than 30 mesh
1	Precalcined Greer	20°C, air	4	10
2	Precalcined Greer	870°C, air	6	11
3	Greer	870°C, air	6	14
4	Greer	870°C, 0.3% SO_2, bal. air	11	15
1	Precalcined Tymochtee	20°C, air	16	27
2	Precalcined Tymochtee	870°C, air	9	21
3	Tymochtee	870°C, air	10	23
4	Tymochtee	870°C, 0.3% SO_2, bal. air	3	10
1	Precalcined 2203	20°C, air	41	55
2	Precalcined 2203	870°C, air	92	96
3	Limestone 2203	870°C, air	94	97
4	Limestone 2203	870°C, 0.3% SO_2, bal. air	38	49

limestone in its natural form is very attrition-resistant; the results for Greer for runs (3) and (4) are identical within experimental error.

(4) The extent of sulfation or rate of sulfation is important. Even though Tymochtee dolomite is a softer stone than Greer (compare tests 1, 2, and 3 for Greer and Tymochtee), simultaneous calcination and sulfation of Tymochtee produced a stone that was more attrition-resistant than Greer. This is in agreement with previous results (ANL/CEN/FE-77-3) of attrition studies of Greer and Tymochtee dolomite in the PDU pressurized combustor. Greer limestone and Tymochtee dolomite losses due to attrition and elutriation were 20% and 16%, respectively, for Greer limestone and Tymochtee dolomite.

(5) Some limestones are less attrition-resistant than are dolomites. For example, limestone 2203 is a very soft high-calcium stone (96% $CaCO_3$).

(6) Composition may be important. Large quantities of Al, Si, and Fe in stone may produce more attrition-resistant stones. This can only be determined by examining a large number of limestones and dolomites (ANL/CEN/FE-77-3).

(7) Other limestone physical properties such as grain size and grain defects are important. As shown previously (ANL/CEN/FE-77-3), limestones with similar compositions can have widely different attrition rates.

5. Carbon Burnup Cell Studies

(R. B. Snyder, E. B. Smyk, R. L. Beaudry, and J. R. Falkenberg)

The sulfur retention at carbon burnup cell (CBC) conditions has been estimated, using previously reported TGA data. The results suggest that 60-80% SO_2 retention may be possible. To further investigate this, studies were intiated, using as a carbon burnup cell a PDU combustor having a 10.8-cm diameter and a 46-cm bed height.

Typical CBC results for one analyzer are given in Table 5 and results for two analyzers showing the uncertainty in SO_2 retention are given in Fig. 2. The CBC was operated at temperatures between 850 and 1100°C with the bed fluidized. At 850°C with Greer limestone and Sewickley coal (4.3% S), approximately 88% sulfur retention was obtained (Ca/S = 12) in good agreement with a TGA estimate of 93%. At 1000 and 1050°C, SO_2 retention decreased to 70 and 55% (Fig. 2), respectively. Sulfur retention dropped rapidly between 1050 to 1100°C. At 1100°C, SO_2 retention ranged from 0 to 6% (Fig. 2). This disagreed with TGA results, which projected retention of 85% of the SO_2.

When sulfated Greer limestone (8.2% S) was used at 850°C (CaO/S = 11.4), 84% of the SO_2 was retained (Fig. 2). However, above 1050°C, partial regeneration of the sulfated Greer limestone occurred. At 1100°C, approximately 20% of the $CaSO_4$ in the sulfated Greer was converted to CaO, producing approximately 4400 ppm SO_2 in the off-gas.

By use of sulfated Tymochtee dolomite (7% S) at 850°C approximately 90% of the SO_2 was retained (Fig. 2). Retention of SO_2 decreased to 76, 35, and 6% at 1000, 1050, and 1100°C, respectively. The sulfated Tymochtee performed better than sulfated Greer and essentially the same as fresh Greer limestone. This suggests that release or capture of SO_2 at the operating temperature of 1100°C is dependent upon the type of $CaSO_4$-bearing material used.

Normal CBC operation will use combustor overhead material ("fly ash"). Since this material is somewhat different from the materials fed in runs 16a-22, overhead material from the 15.2-cm-ID pressurized combustor was tested. Due to the low heating value of 3000 Btu/lb, for this overhead material and its small particle size, it was not possible to sustain the desired temperatures. Char was added to increase the heating value of the fuel. Nevertheless, it was still impossible to control the reactor at 1100°C. The small particles became entrained in the fluidizing gas; within 5 min, they plugged the off-gas filters, causing the pressure to increase and preventing operation of the combustor.

6. Enhancement of Limestone Sulfation

(J. A. Shearer and C. B. Turner)

The enhancement of sulfation of limestones in an FBC environment by the addition of inorganic salts can greatly reduce the quantities of stone necesary to meet EPA air pollution standards for sulfur emitted from fluidized-bed coal combustors. In particular, results reported earlier (ANL/CEN/FE-78-3) on the effect of $CaCl_2$ on a few select stones showed much greater sulfation than for NaCl with trace amounts of salt added ($\leq$0.5 mol %).

Table 5. Process Development Unit Carbon Burnup Cell Tests

Run No.	Temp., °C	Bed Material	Superficial Gas Velocity, m/s	O_2 in Off-Gas, %	Calc. SO_2 from Sewickley Coal[a], ppm	SO_2, ppm	SO_2 Retention, %
12	1100	Sand	2.6	8.6	2450	2500	0
16a	850	Greer	1.6	13.5	1475	300	80
16b	1050	Greer	1.6	8.5	2350	1150	51
17a	1000	Greer	1.7	8.8	2300	1000	57
17b	1100	Greer	1.7	6.2	2800	3000	0
17c	1100	Greer	1.6	6.7	2700	3000	0
18a	850	Sulfated Greer[b]	1.7	13.5	1475	300	80
18b	1000	Sulfated Greer	1.7	10.5	2000	1200	40
18c	1050	Sulfated Greer	1.7	9	2250	2200	3
18d	1100	Sulfated Greer	1.7	6.4	2750	4800	c
19	850	Sulfated Tymochtee[d]	1.7	11.8	1750	300	83
20a	1000	Sulfated Tymochtee	1.7	9.0	2270	600	74
20b	1050	Sulfated Tymochtee	1.7	8.0	2450	1450	41
22	1100	Sulfated Tymochtee	1.7	8.3	2400	2200	8

[a] ppm SO_2, assuming that all sulfur in the coal was converted to SO_2 and was present in the off-gas.

[b] Sulfated Greer limestone contained 8.2% S.

[c] Regeneration of 15-25% of the sulfated Greer occurred.

[d] Sulfated Tymochtee contained 7% S.

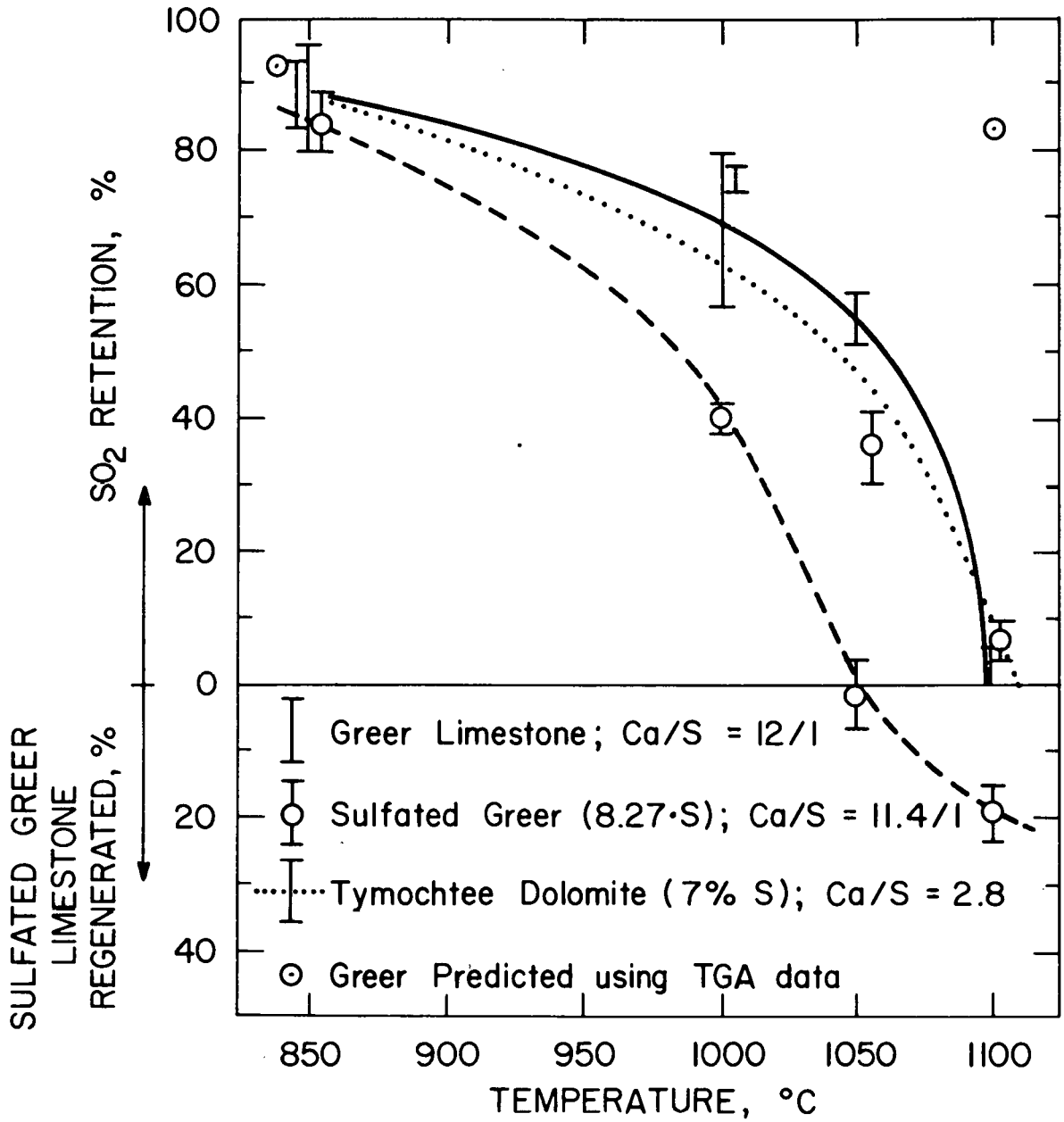

Fig. 2. SO_2 Retained in a Carbon Burnup Cell

During this report period, a large number of limestones, with added $CaCl_2$, representing considerable variation in compositions and morphologies were reacted with a simulated flue gas in a tube furnace. The flue gas consisted of 0.3% SO_2, 5% O_2, 20% CO_2, and the balance N_2. Reaction was carried out at 850°C for 6 h, using either untreated stones or stones treated with an evaporated aqueous solution of $CaCl_2$. Chemical analyses for the virgin stones are listed in Table 6. Results for sulfation experiments carried out with these limestones are presented in Table 7 as percent of CaO converted to $CaSO_4$. Data are presented for untreated stones, limestones treated with 0.1 mol % $CaCl_2$, and stones treated with 0.5 mol % $CaCl_2$. As suggested by the results of earlier work, (ANL/CEN/FE-78-3), maximum conversions to sulfate are achieved with $CaCl_2$ additions of $\leq$0.5 mol %; comparison of Tables 6 and 7 shows that larger quantities of salt are generally required for stones having the greatest impurity content. In almost all cases, except with some very pure limestones, the maximum conversion to sulfate approaches 50-60%. Even in these pure stones, reactivity increases substantially in comparison to no treatment.

The amounts of $CaCl_2$ required are so small that this salt appears more promising than NaCl (which requires $\geq$1.0 mol % as a sulfation enhancer). In FBCs, the introduction of major amounts of corrosive species is to be avoided. Also indicating the desirability of $CaCl_2$ is that it is used routinely as a freeze-proofing material for coal storage piles in quantities comparable to those used in this work with no apparent major corrosive effects. In a program paralleling this sulfation enhancement work, a series of steels are being exposed to a simulated flue gas that has passed through a bed of $CaCl_2$ containing limestone, followed by metallographic analysis of the steels to determine any corrosive effects (ANL/CEN/FE-78-5).

The effects of $CaCl_2$ on the calcined limestone are similar to the effects of NaCl addition. When either salt is added to the limestone during calcination, the average pore diameters of the calcines increase. Representative curves are presented later in this report. $CaCl_2$ is slightly more effective than NaCl in terms of increasing the pore diameters, and smaller amounts of $CaCl_2$ than of NaCl are required to produce the same magnitude of shift. The porosity reaches an optimum pore size distribution with respect to sulfation with small additions of $CaCl_2$. The maximum sulfation reactivity occurs near 0.3 μm, as shown in Fig. 3, which plots "average" pore diameter *vs.* percent conversion for a selected few stones treated with various amounts of $CaCl_2$. The average pore diameters were calculated from surface areas and volumes for those pores larger than or equal to 0.01 μm since smaller pores are ineffective in sulfation. The range of pore size distributions resulting in optimum sulfation reactivity using $CaCl_2$ is the same range observed to give optimum reactivity for NaCl addition. This supports the concept that pore size and distribution constitute the major controlling factors determining the extent of sulfation of limestones in SO_2/O_2 mixtures for particles averaging 18-20 mesh.

In continuing the study of the effects of different salts, $MgCl_2$ was used and was found to be an effective enhancer of limestone sulfation at very low concentrations. Table 8 lists the percent conversions of available CaO to $CaSO_4$ for four limestones treated with $MgCl_2$ (introduced via evaporation from an aqueous slurry). The same effect is present (high conversions at both low and high additive concentrations) as was observed for $CaCl_2$ (ANL/CEN/FE-78-3). In the low-$MgCl_2$-concentration region ($\leq$0.5 mol %), porosity changes occur that are favorable to sulfation via trace amounts of a liquid phase.

Table 6. Wet Chemical Analyses[a] of Virgin Stones

Limestone Designation	$CaCO_3$, wt %	$MgCO_3$, wt %	Fe_2O_3, wt %	Al_2O_3, wt %	SiO_2, wt %	Na_2O, wt %	K_2O, wt %	
ANL-7401	74.7	10.2	1.07	1.82	11.20	0.19	0.36	99.54
ANL-8001	80.4	3.5	1.24	3.18	10.34	0.23	0.72	99.61
ANL-8101	81.6	11.6	0.86	0.19	1.86	0.10	0.07	96.28
ANL-8301	83.9	13.4	0.14	0.42	1.24	0.02	0.02	99.14
ANL-8701	87.0	1.20	3.4	2.0	7.1	<0.13	0.19	101.02
ANL-8903	89.3	1.21	0.98	0.83	5.5	0.12	0.22	98.16
ANL-8902	89.6	3.02	0.37	0.79	5.06	0.03	0.29	99.16
ANL-8901	89.8	2.15	0.66	1.04	4.00	0.10	0.19	97.94
ANL-9201	92.6	5.33	0.20	0.42	1.26	0.10	0.02	99.93
ANL-9401	94.1	1.00	0.35	0.51	3.18	0.05	0.10	99.29
ANL-9501	95.3	1.32	0.09	0.25	0.77	0.03	0.06	97.82
ANL-9504	95.8	0.58	0.30	0.36	2.71	0.05	0.13	99.88
ANL-9601	96.0	3.57	0.23	0.01	0.18	0.04	0.01	100.04
ANL-9701	97.8	0.6	0.10	1.8	0.2	0.25	0.47	101.22
Calcite	100.0	0.0	0.0	0.0	0.0	0.0	0.0	100.00

[a]Analyses performed by Analytical Chemistry Laboratory, ANL.

Table 7. Sulfation of Limestone with Added $CaCl_2$ at 850°C in 6 h. 0.3% SO_2, 5% O_2, 20% CO_2, and the balance N_2

	CaO To $CaSO_4$, % Conversion		
Limestone Designation	Untreated Blank	With 0.1 mol % $CaCl_2$	With 0.5 mol % $CaCl_2$
ANL-7401	41.5	48.6	65.2
ANL-8001	38.0	49.3	52.8
ANL-8101	33.5	49.9	40.7
ANL-8301	29.3	42.7	59.9
ANL-8701	33.2	50.3	59.4
ANL-8903	43.0	55.4	30.0
ANL-8902	29.9	49.0	47.4
ANL-8901	30.0	43.7	46.6
ANL-9201	28.1	43.9	30.5
ANL-9401	51.7	56.3	30.0
ANL-9501	13.0	50.0	28.5
ANL 9504	25.9	44.2	35.4
ANL-9601	30.0	36.7	46.0
ANL-9701	7.0	35.1	32.7
Calcite	5.2	35.0	30.0

Table 8. Conversion to Sulfate in 6 h with 0.3% SO_2 at 850°C for Limestones Precalcined with $MgCl_2$ Additive at 850°C, 1 h in 5% O_2, 20% CO_2, and the Balance N_2.

Limestone	$MgCl_2$ Added,[a] mol %	CaO to $CaSO_4$, % conversion
ANL-8001 (Greer) (∿20% Impurities)		
	0.0	38.0
	0.1	49.2
	0.5	54.7
	1.0	57.0
	4.0	41.3
	5.0	48.5
ANL-8903 (∿9% Impurities)		
	0.0	43.0
	0.1	57.9
	0.5	45.6
	1.0	33.9
	4.0	52.4
ANL-9501 (Grove) (∿4% Impurities)		
	0.0	13.0
	0.1	28.4
	0.5	36.6
	1.0	20.9
	4.0	32.9
Calcite Spar (∿0% Impurities)		
	0.0	5.2
	0.1	24.0
	0.5	25.7
	1.0	21.0
	4.0	36.8

[a] $MgCl_2$ was introduced via evaporation from an aqueous slurry.

Intermediate amounts of $MgCl_2$ (1-2 mol %) decrease the reactivity of the stone. Higher concentrations (>2 mol %) result in large amounts of a liquid phase forming, with substantial amounts of dissolved CaO accelerating the formation of $CaSO_4$.

With respect to the magnitude of the effect of $MgCl_2$ in comparison with NaCl and $CaCl_2$ during calcination, Figures 4, 5, and 6 show porosity curves for four limestones treated with (1) NaCl, (2) $CaCl_2$, and (3) $MgCl_2$, respectively. The horizontal bars with arrowheads mark the extent to which pore diameters of the majority of pores shifted when 0.5 mol % salt was added to untreated stones. In all three graphs, the effect of salt is greatest for the purest limestone, decreasing as the impurity content increases.

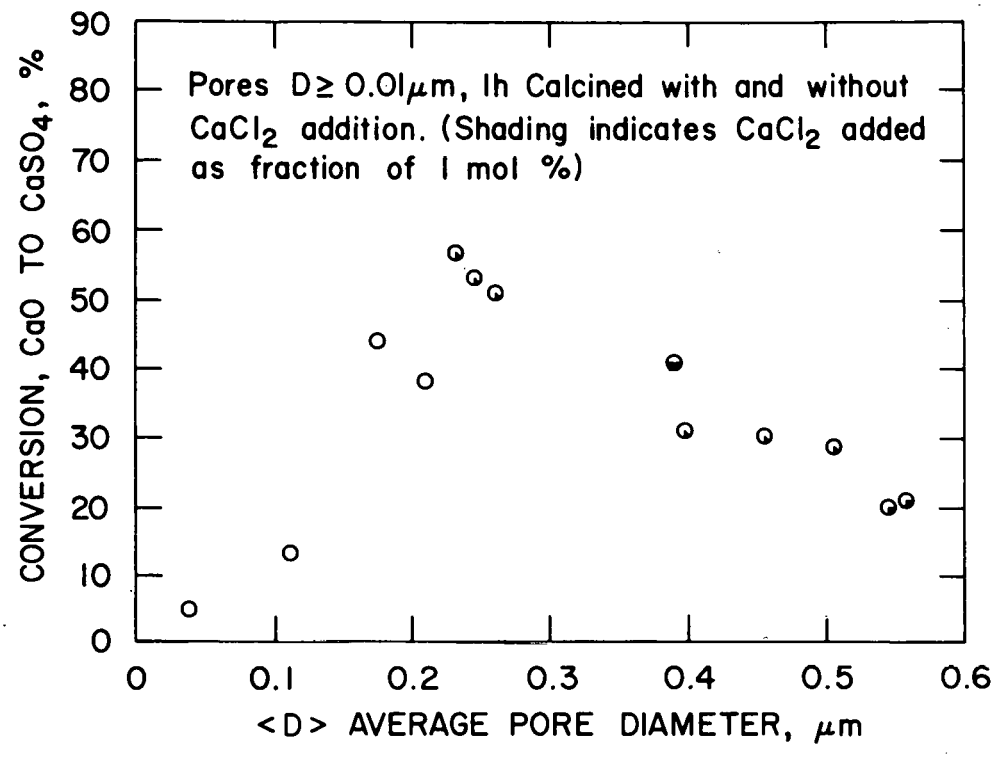

Fig. 3. Percent Conversion to Sulfate vs. Average Pore Diameter for Four Limestones Sulfated at 850°C, 5 h in 0.3% SO_2, 5% O_2, 20% CO_2, and the balance N_2 calcined 1 h with and without $CaCl_2$ Addition.

As a result, effects on ANL-8001 with ∿20% impurities are very small. The relative order of effectiveness of the three salts for a given mol percent salt is $MgCl_2$ > $CaCl_2$ > NaCl. In terms of weight percent addition, $MgCl_2$ and $CaCl_2$ are comparable. Much less of either is required than of NaCl. Most of the treated limestones show an increase in the total porosity at 0.5 mol % salt (in comparison to porosities of the untreated stones) as well as a shift to larger average pore diameters.

Concurrently with the $CaCl_2$ and $MgCl_2$ work, the effects of other inorganic salts were studied. Table 9 lists percent conversions to $CaSO_4$ for four limestones treated with a variety of salts each of which was added to give a concentration of 1 mol %. Related to our interpretation of these data is our understanding of the effects of NaCl and $CaCl_2$--it has become apparent that maximum effects cannot be found by using only one concentration of salt in a single sulfation experiment. Porosity curves at several salt concentrations can be used to determine the concentration of a salt most likely to give maximum reactivity with SO_2/O_2, based on the assumption that there is an optimum pore distribution for limestone sulfation, regardless of composition. Once this salt concentration is found, a series of bracketing sulfation experiments should serve to indicate the maximum sulfations achievable for the particular stone and salt used. Nevertheless, the data in Table 9 show that

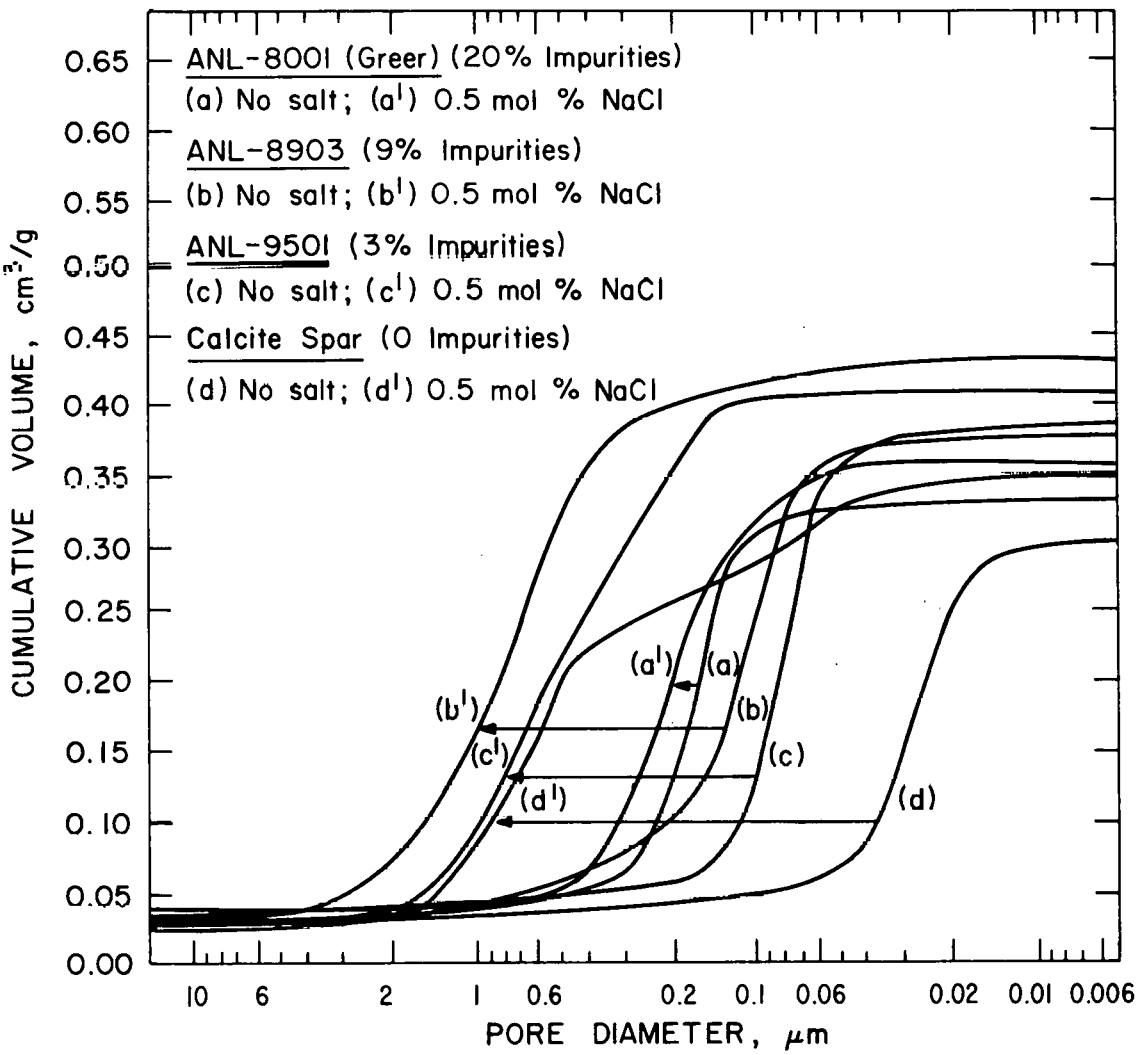

Fig. 4. Changes in Porosity upon Addition of 0.5 mol % NaCl to Limestones Calcined at 850°C, 1 h, in 5% O_2, 20% CO_2, and the balance, N_2.

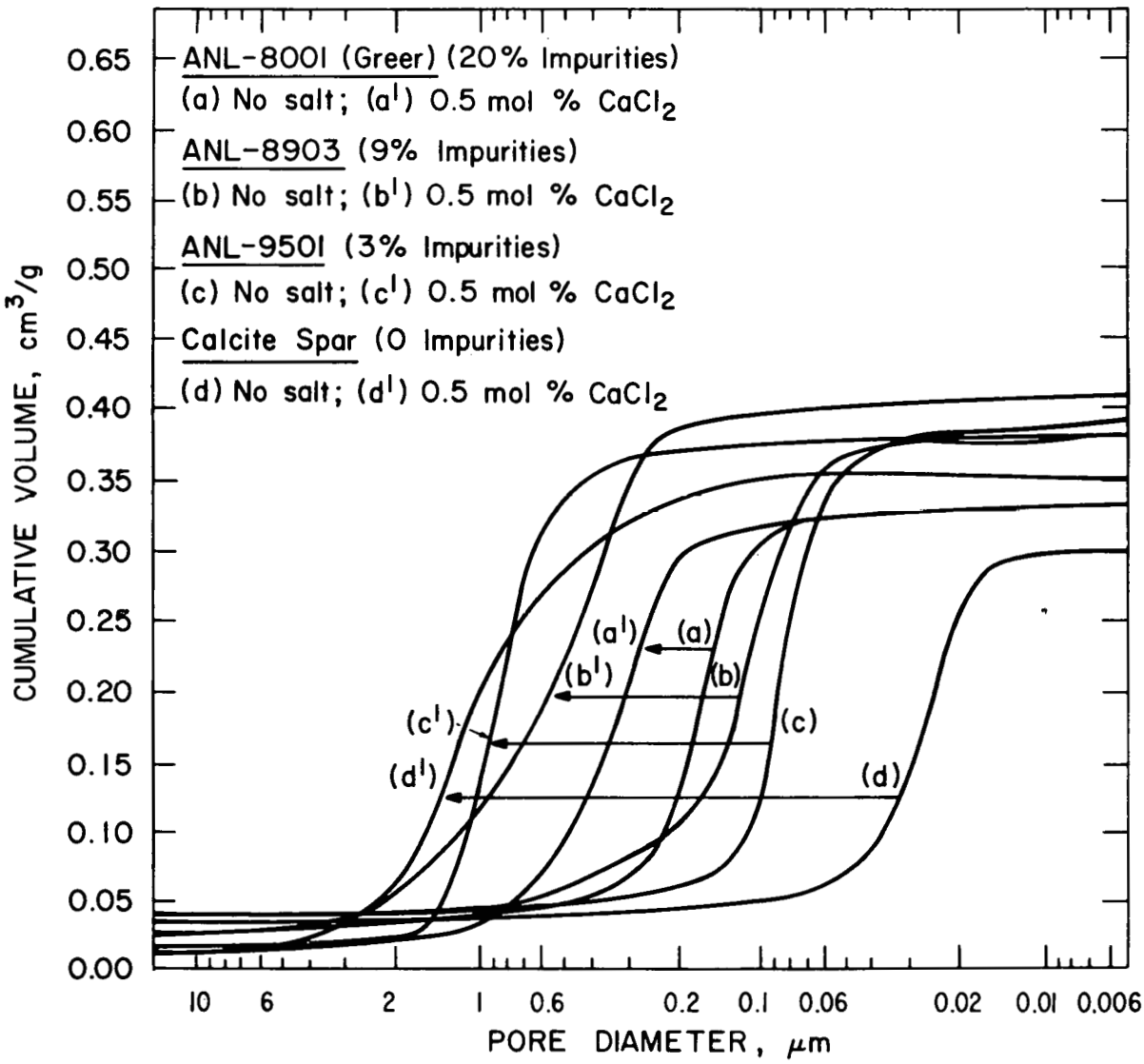

Fig. 5. Changes in Porosity upon Addition of 0.5 mol % $CaCl_2$ to Limestones Calcined at 850°C, 1 h, in 5% O_2, 20% CO_2, and the balance N_2.

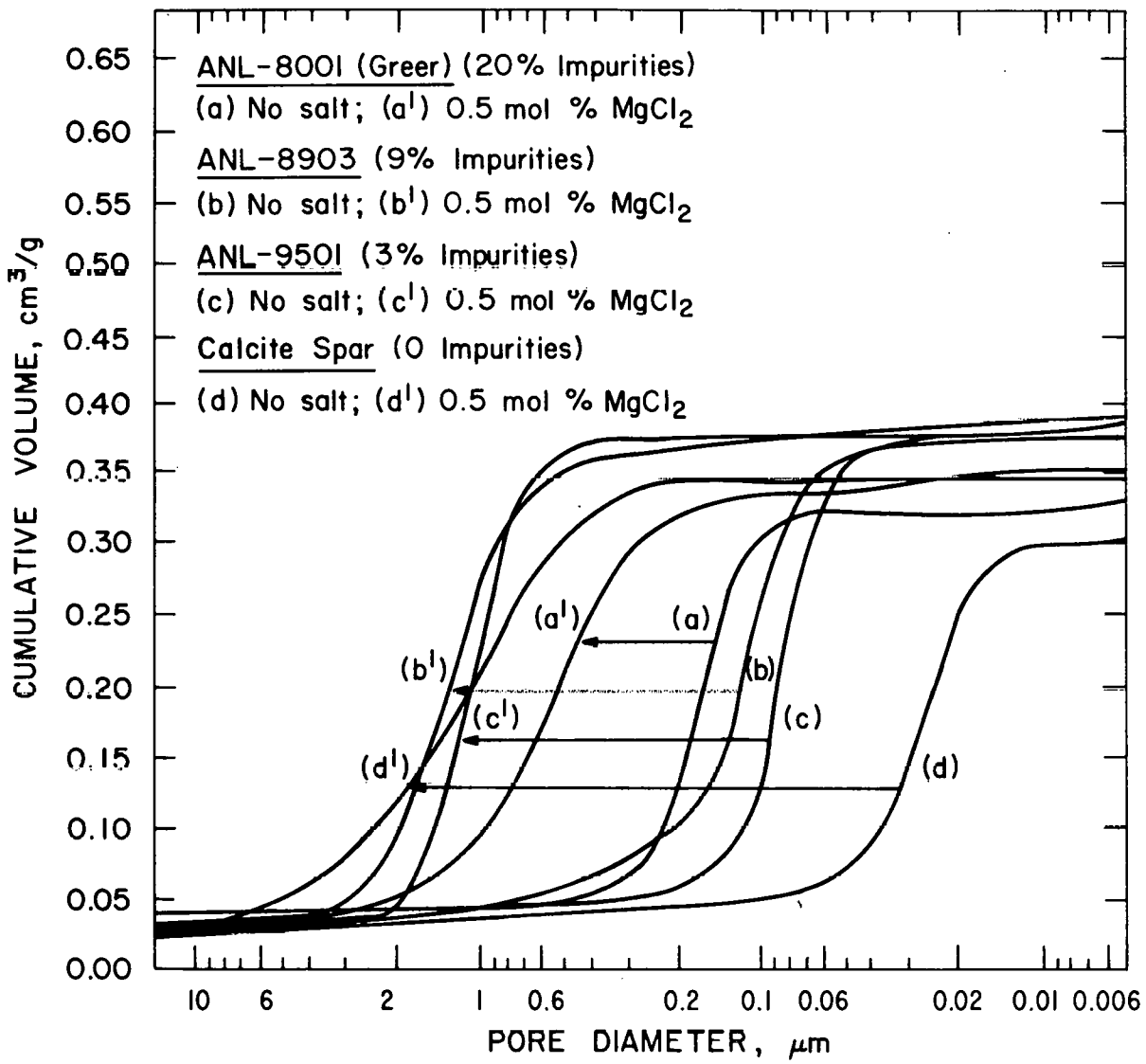

Fig. 6. Changes in Porosity upon Addition of 0.5 mol % $MgCl_2$ to Limestones Calcined at 850°C, 1 h in 5% O_2, 20% CO_2, and the balance N_2.

Table 9. Conversion to Sulfate after 6 h with 013% SO_2 at 850°C for Limestones Precalcined with Inorganic Additives (1 mol %) at 850°C, 1 h in 5% O_2, 20% CO_2, and the balance N_2.

Additive	Calcite Spar, No Impurities	ANL-9501 (Grove), ∿4% Impurities	ANL-8903, ∿9% Impurities	ANL-8001 (Greer), ∿20% Impurities
Untreated	5.2	13.0	43.0	38.0
NaCl	33.3	44.4	47.5	43.9
NaOH	20.2	27.6	43.5	41.0 pos. effect
Na_2CO_3	23.6	43.6	41.0	40.0 pos. effect
Na_2SO_4	23.8	41.5	43.2	46.8 pos. effect
Na_2SiO_3	5.2	12.3	48.4	40.3
$Na_2SiO_3 \cdot 9H_2O$	21.4	36.8	39.8	44.9
$CaCl_2$	19.2	19.9	34.7	50.6
$MgCl_2$	21.0	20.9	33.0	54.7
$Ca(OH)_2$	10.4	12.4	47.5	49.0
CaF_2	20.6	26.3	53.6	45.8
$CaSO_4$	8.0	13.6	44.4	46.1
H_3BO_3	5.1	17.3	43.9	46.8

Early Qualitative Results

most of the salts tested have measurable effects either positive or negative. Hence all are potential sulfation-enhancers at proper salt concentrations.

The number of limestone types studied is being increased (1) to verify that these effects occur for many possible combinations of stone composition and morphology and (2) to reduce significant statistical error in sampling and in making correlations in general. Both sulfation and porosity measurements on untreated and salt-treated stones are required.

TASK B. TURBINE CORRODENT STUDIES

1. Removal of Alkali Metal Compounds from Hot Flue Gas of Coal Combustion (S. Lee and D. Fredrickson)

In the prospective application of pressurized fluidized-bed combustion of coal for power generation, a potential problem to be solved is corrosion of turbine blades (in a gas turbine downstream from the fluidized-bed combustor) due to the attack of alkali metal compounds in the hot flue gas. This problem can be eliminated by reducing the concentration of alkali metal compounds in the hot flue gas to a level tolerable for a turbine blade. A way of accomplishing this is to remove the alkali metal compounds* from the hot flue gas in a hot fixed-bed sorbent filter before the gas is expanded into a turbine. The objective of this task is to develop an effective sorbent for use in a hot fixed-bed sorbent filter.

a. Removal of Sodium Chloride with Activated Bauxite and Diatomaceous Earth

Experimental results presented in the previous report of this series (ANL/CEN/FE-78-3) showed that diatomaceous earth, activated bauxite, and kaolin clay effectively remove both NaCl and KCl vapors from simulated dry flue gas of PFBC. Systematic studies have been carried out in this report period to investigate the effects of some operating variables on the sorption performance of two of these sorbents. Results of a series of experiments to examine the effect of sorbent bed temperature on the sorption capability of diatomaceous earth and activated bauxite for NaCl vapor are presented below.

Table 10 gives the experimental conditions for this series of experiments. The sorption capability of a sorbent can be affected to different degrees by several operating variables [such as bed temperature, pressure, alkali metal compound vapor concentration in the flue gas, linear velocity and hourly gas space velocity (GHSV) of the flue gas, etc.]. Until these variables are fully studied, the magnitudes of their effects on the sorption capability of a sorbent can only be estimated. To effectively examine the effect of one variable (sorbent bed temperature in this work) within a reasonable experimental time, the other variables have to be constant and their effects on the sorption capability of a sorbent should be theoretically minimized to prevent their masking the effect of the variable being observed; therefore, as shown in Table 10, a fairly thin bed of sorbent and high GHSV were chosen. These conditions also allowed better control of the bed temperature (the variable observed). The GHSV is related to the rate of flue gas throughput through the bed; the reciprocal of it is the contact time of the flue gas with the sorbent. The contact time for this series of experiments was on the order of 0.05 s.

In this series of experiments, 15 and 30 g of diatomaceous earth and activated bauxite sorbents, respectively, was tested in each run. The accuracy of the measured sodium content in the sorbent depends on the method of obtaining a representative sample of the sorbent for analysis. The experimental procedures for analyzing the sodium content in the sorbent were as follows: Representative samples of the sorbent for analysis were obtained by

*Removal of all particulates from flue gas is being studied in Task D.

Table 10. Experimental Conditions for Testing Diatomaceous Earth and Activated Bauxite for NaCl Vapor Capture.

Avg. Sorbent-Bed Temp.	800 and 880°C
System Pressure	100 kPa
Particle Size of Sorbent	-8 +10 mesh
Thickness of Sorbent Bed	1.3 cm
Flowing Gas Composition	3% O_2 16% CO_2 300 ppm SO_2 Balance N_2
Gas Flow Rate	11.3 L/min
Linear Velocity of Flowing Gas through the Bed	24 cm/s at 800°C
GHSV (hourly gas space velocity)	67000 at 800°C
NaCl Vapor Concentration in Flowing Gas at Sorbent Bed Inlet	69 to ∿98 ppm

[a]In a run, preheated synthetic flue gas enters the horizontal combustor vessel, passes over the alkali metal compound which is vaporized by induction heating, passes through heated sorbent retained by two pieces of platinum gauze inside the filter bed container, passes over a cold trap, and finally passes through a glass wool filter which serves as a backup for the cold trap.

first grinding the entire amount of the sorbent tested to about -100 mesh powder. After thorough mixing of the powder, represnetative samples (one-gram samples for diatomaceous earth and one-half-gram samples for activated bauxite) were taken for further preparation of analysis solutions. Diatomaceous earth samples were each dissolved in a mixture of concentrated H_2SO_4, HF, and HNO_3 according to the method used by Bureau of Mines.[2] For activated bauxite, the sample was fused with NH_4HF_2 and then dissolved in slightly acidified distilled water. The resulting solutions were analyzed for sodium, using flame emission spectrometry.

Tables 11 and 12 show the material balances of NaCl from the testing of diatomaceous earth and activated bauxite, respectively, for NaCl vapor capture as a function of sorbent bed temperature and duration of the experiments. Since total NaCl vapor transported in the 880°C series of experiments was substantially higher than that in the 800°C series the sorption capacities from the 880°C series were recalculated to an 800°C basis and are given in parentheses in row 3 of both tables. These were used in plots (Fig. 7) to allow the sorption capacity to be compared at the same basis.

Table 11. Distributions of NaCl with NaCl Vapor Capture by Diatomaceous Earth as a Function of Temperature and Experiment Duration. In each experiment, 15.0 g sorbent was tested at atmospheric pressure in a simulated dry PFBC flue gas at a linear velocity of 25 cm/s and GHSV=67,000 h^{-1} at 800°C.

	Experiment							
	HGC-19	HGC-21	HGC-20	HGC-34	HGC-22	HGC-23	HGC-24	HGC-29[a]
Sorbent Bed Temperature, °C	880	880	880	880	800	800	800	800
Experimental Time, h	1	2	3	4.5	1	2	3	6
	Total NaCl, mg							
(1) NaCl Collected by								
(a) Cold Trap	7	27	65	95	5	42	56	182
(b) Glass Wool Filter	3	15	37	47	2	9	31	107
(2) NaCl Captured by Sorbent[b]	129	296	388	516	124	251	343	544
(3) Total	139	338	490	658	131	302	430	833
(4) Sorption Capacity, mg NaCl/g sorbent [(2)/15]	8.6 (8.1)[c]	19.7 (17.6)[c]	25.9 (22.7)[c]	34.4 (32.9)[c]	8.3	16.7	22.9	36.3

[a] The system pressure increased to 146 kPa at the end of the experiment. This was because the glass wool filter gradually became compacted owing to the high flow.

[b] Sodium concentrations of the sorbent were obtained by dissolving representative samples of sorbent in a mixture of H_2SO_4, HF, and HNO_3, and then analyzing the solution using the flame emission spectrometry (FE). FE analysis was done by R. Bane.

[c] Values that would be obtained if the corresponding amounts of NaCl vapor were transported as in the 800°C series of experiments. For example, 8.1 was obtained from $131 \times \frac{129}{139}/15$.

Table 12. Distributions of NaCl with NaCl Vapor Capture by Activated Bauxite as a Function of Temperature and Experiment Duration. In each experiment, 30.0 g sorbent was tested at atmospheric pressure in a simulated dry PFBC flue gas at a linear velocity of 25 cm/s and GHSV=67,000 h^{-1} at 800°C.

	Experiment							
	HGC-25	HGC-26	HGC-27	HGC-28[a]	HGC-30	HGC-32	HGC-31	HGC-33[a]
Sorbent Bed Temperature, °C	800	800	800	800	880	880	880	880
Experimental Time, h	1	2	3	6	1	2	3	4.5
	Total NaCl, mg							
(1) NaCl Collected by								
(a) Cold Trap	6	22	40	160	16	38	106	180
(b) Glass Wocl Filter	4	10	22	100	6	19	58	103
(2) NaCl Captured by Sorbent[b]	170	343	444	734	c	c	c	c
(3) Total	180	375	506	994				
(4) Sorption Capacity, mg NaCl/g sorbent [(2)/30]	5.7	11.4	14.8	24.5				

[a]System pressure increased to 169 kPa at the end of the experiments. This was because the glass wool filter gradually became compacted owing to the high flow.

[b]Sodium concentration of the sorbent was obtained by fusing representative samples of the sorbent with NH_4HF_2, dissolving the samples in distilled water, and then analyzing the solutions using flame emission spectrometry (FE). FE analysis was done by R. Bane.

[c]Analyses not yet completed.

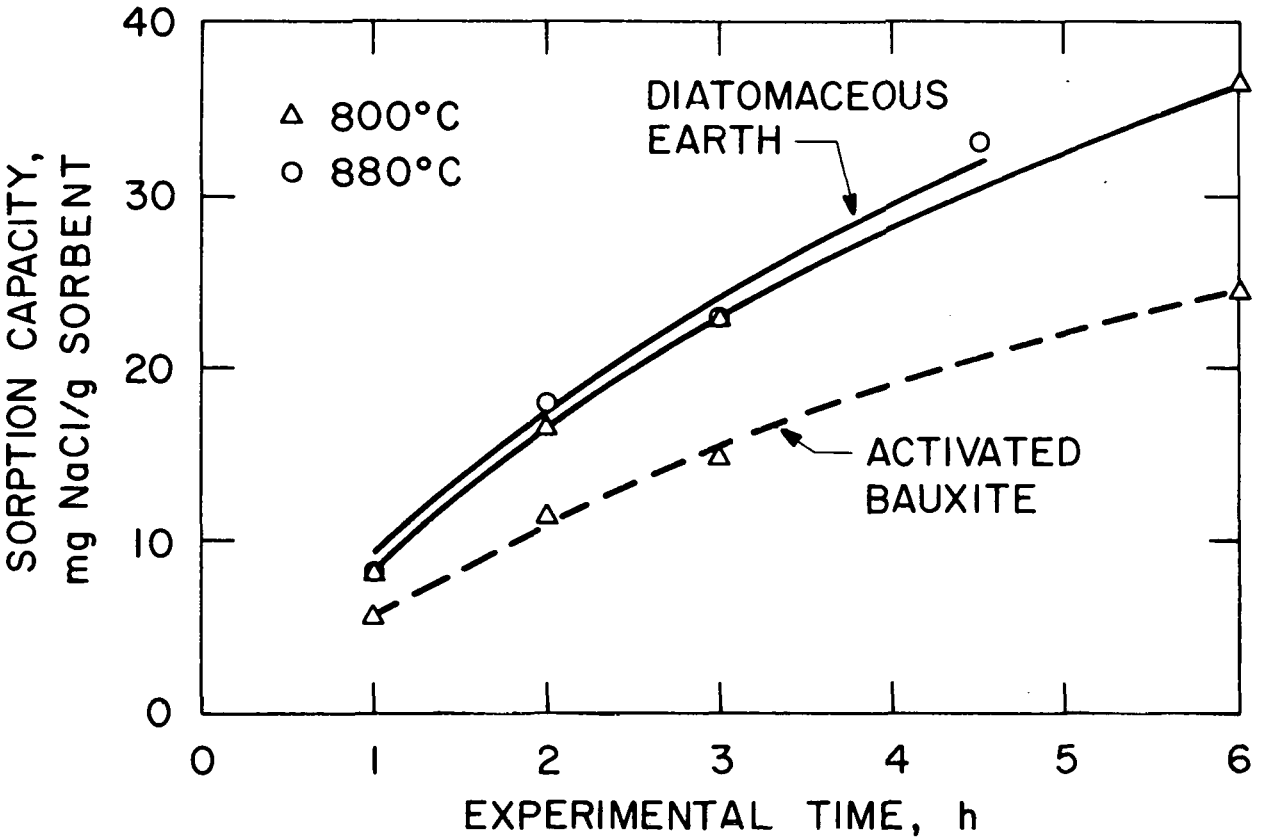

Fig. 7. Effect of Sorbent Bed Temperature on Sorption Capacity as a Function of Experimental Time. Experimental data for 880°C was adjusted to be on the same basis as the 800°C data.

As can be seen in Fig. 7, the sorption capacity of diatomaceous earth is greater than that of activated bauxite on a weight basis (*i.e.*, milligrams of NaCl per gram of sorbent). This is due to activated bauxite being more dense than diatomaceous earth. In all of these experiments, a 1.3-cm-thick bed was packed with sorbent; on a volume basis (*i.e.*, milligrams of NaCl per milliliter of sorbent), the sorption capacities of activated bauxite are greater than those of diatomaceous earth.

As shown in Fig. 7, the sorption capacity of diatomaceous earth increases at the higher sorbent bed temperature. This indicates that the reaction rate between NaCl vapor and diatomaceous earth is probably endothermic. Figure 7 also shows that the sorption capacities of both diatomaceous earth and activated bauxite increase nonlinearly with experimental time. This suggests that under the experimental conditions, the reaction rate for NaCl and diatomaceous earth and the adsorption rate of NaCl on activated bauxite are not controlled by the mass transfer of NaCl vapor from the bulk of flue gas to the external surface of the sorbent.[3]

The effect of the linear velocity of the flue gas passing through the bed is to be studied because it affects not only the mass transfer phenomenon, but also is an important parameter in designing a sorber. For a given volumetric flow rate of flue gas, the linear gas velocity determines the bed cross-sectional area of a sorber. To study the effect of the linear gas

velocity on the sorption capacity of both diatomaceous earth and activated bauxite at high linear velocities, a bed container with a smaller cross section than the one presently used is being used. This is necessary because there is a limit to the gas flow rate that can be passed through a combustor without substantially increasing the system pressure. Two filter bed containers with small cross sections have been fabricated. One container will allow a linear gas velocity of 66 cm/s (or 26 in./s), the other 155 cm/s (or 61 in./s). A series of tests is being conducted at these high linear gas velocities.

b. Apparatus for Removal of Alkali Metal Sulfates

So far, both diatomaceous earth and activated bauxite have been shown to be very effective sorbents for capturing both NaCl and KCl vapors present in simulated dry flue gas of PFBC. Sodium and potassium as sulfates are also expected to be present in the flue gas from coal combustion. Hot corrosion in a gas turbine is caused by alkali metal sulfates present as liquid films on metal surfaces. Therefore, for a sorbent to be a candidate for removing alkali metal compounds from hot flue gas of coal combustion, its ability to retain alkali metal sulfates has to be demonstrated. Because alkali metal sulfates have substantially lower vapor pressures than their chlorides, and because the allowable maximum operating temperature of the laboratory-scale fixed-bed combustor vessel (presently used for NaCl and KCl vapor sorption tests) is limited to 900°C, the sorption capability of the sorbents for alkali metal sulfates cannot be determined using that combustor. A small-scale sorption test rig that can be operated up to 1250°C has been assembled. Figure 8 is a schematic diagram of the apparatus.

In this test rig, a known amount of alkali metal sulfates in a platinum sample pan is vaporized inside a pure Al_2O_3 tube that is heated by a tubular furnace. A stream of preheated synthetic PFBC flue gas carries the alkali metal sulfate vapor downstream through (1) a bed of the sorbent to be tested and (2) a condenser. Finally, the gas is vented to an exhaust. The sorbent bed is supported by a platinum gauze and quartz tubing that is inserted concentrically inside the Al_2O_3 tube. The Al_2O_3 tube is capped on both ends with lava end caps. Ceramic fiber provides the seal between the Al_2O_3 tube and the end caps. The temperatures of the sample and the sorbent bed are measured with thermocouples. At the end of an experiment, the weight of alkali metal sulfate residue is measured, and the sorbent is analyzed for alkali metal to determine the sorption capacity of the sorbent.

The temperature profile along the center of the Al_2O_3 tube is presently being measured and adjusted. From this, a position of a sorbent bed will be determined that will allow the bed temperature to be controlled within the planned test range (800 to 900°C). Systematic study in which this test rig will be used is expected to start soon.

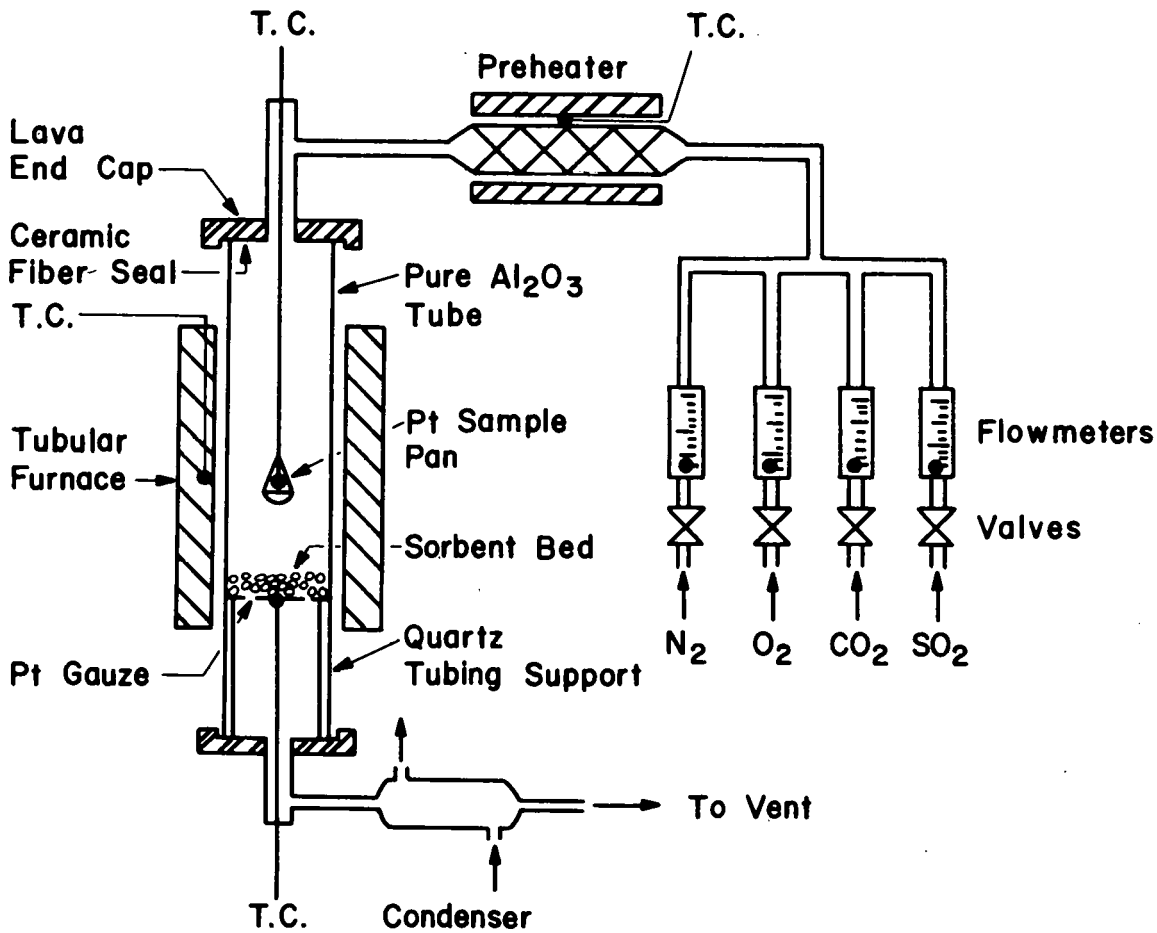

Fig. 8. Apparatus for Study of Sorption of Alkali Sulfates

TASK D. PARTICULATE CONTROL STUDIES

W. Swift, G. Teats, S. Smith, and J. Stockbar

In PFBC, the hot flue gas from the combustor must be expanded through a gas turbine to recover energy and make the process economic. To prevent possible corrosion and erosion of the turbine hardware by particulate matter entrained in the flue gas, the particle loading must be reduced to acceptably low levels. An experimental program is under way at ANL to test and evaluate promising flue gas cleaning methods in the flue-gas system of the 15.2-cm-dia fluidized-bed combustor. Control methods being investigated include acoustic dust conditioning (*i.e.*, agglomeration), a high efficiency controlled-vortex cyclone, and a granular-bed filter.*

1. Acoustic Dust Conditioning

Acoustic dust conditioning is a technique to enhance the natural tendency of polydispersed particulates to impact upon each other and agglomerate. Thus, the use of acoustics in controlling fine particle emissions is a process whereby the mean size of the effluent particles is significantly increased (and correspondingly their number is decreased) by exposure to high-intensity finite-amplitude acoustic fields. As described, acoustic dust conditioning is designed to increase the collection efficiency of downstream duct collectors.

Work is currently being carried out at the University of Toronto to develop and fabricate a pulse-jet acoustic dust-conditioning system consisting of a pulse-jet sound generator, a resonant manifold, and an acoustic-treatment section. A functional description of the components in the system was presented previously (ANL/CEN/FE-77-3). Reported here is the progress made at the University of Toronto toward completion of the fabricated pulse-jet, acoustic dust-conditioning system, which is to be installed in the flue gas system of the ANL 15.2-cm-dia combustor for testing and evaluation.

a. Pulse-Jet Development and Testing at Ambient Pressure

A prototype pulse-jet (Phase I) has been fabricated and assembled on a test bench, as schematically shown in Fig. 9. The test unit was designed to permit the testing of a wide range of geometrical configurations. It was tested at ambient pressure for subsequent testing of a second unit at high pressure. The objectives of the tests are to achieve a high level of sound intensity over a wide range of frequency. The geometrical configurations were varied as follows:

1. Intake and exhaust pipe configurations were varied.
2. Three combustion chambers of similar geometry but different lengths and diameters were examined.
3. Fuel nozzle geometry was varied.

Propane gas was used as the fuel for the pulse-jet.

---

*The use of granular-bed filters to remove alkali metal compounds is being investigated in Task B.

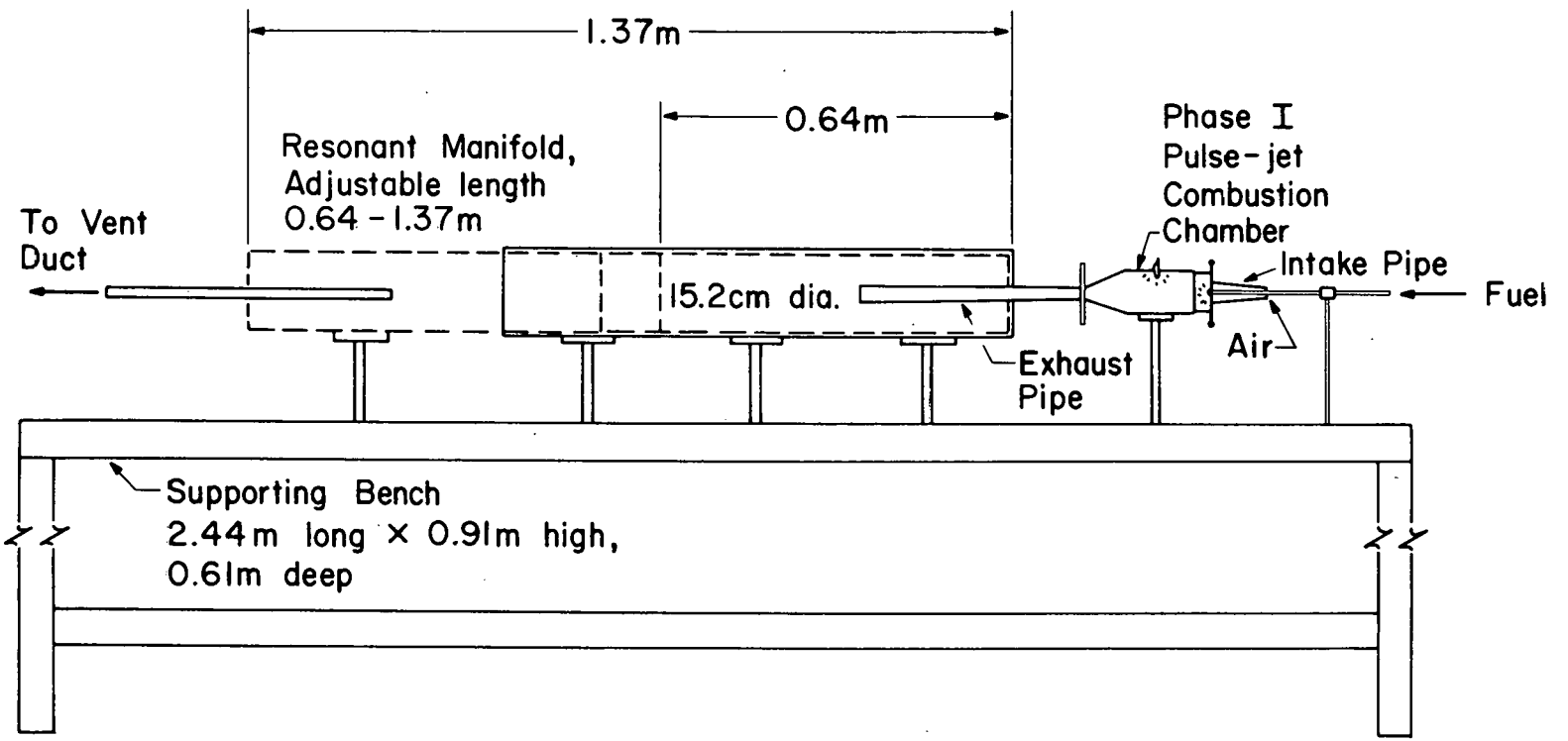

Fig. 9. Pulse-Jet Test Unit Arrangement

Table 13 summarizes the qualitative results obtained during the current series of tests at ambient pressure.

b. Resonant Manifold

Construction of the resonant manifold has been completed. Testing of the unit at ambient pressure is being initiated. Should the acoustic performance of the manifold prove to be satisfactory, the manifold (which is made of heavy gauge steel) will be used for high-pressure testing after the addition of instrumentation fittings. The basic geometry of the resonant manifold is illustrated in Fig. 9.

Table 13. Qualitative Capability of Pulse-Jet Operation at Ambient Pressure

Characteristic	Capability	Comments
Sound Intensity	≤135 dB	Obtained using combustion chamber No. 2, with its exhaust pipe installed at one end of a 0.30-m-dia vent rather than in the resonant manifold duct. The sensing microphone was installed in the wall of the vent duct 3.05 m downstream from the exhaust pipe; the microphone was oriented for gauging of incidence sound values.
Sound Frequency	200 to 450 Hz	Frequency depends on the combined length of the intake pipe, combustion chamber, and exhaust pipe.
Air Intake	--	Operation with or without forced flow of air to the combustion chamber had no effect on sound intensity or frequency.

c. Pulse-Jet Development and Testing at Elevated Pressure

The geometry of the high-pressure pulse-jet will be finalized based on the findings of the tests at ambient pressure. A combustion chamber (No. 4) has been fabricated (Phase II) that is a direct copy of combustion chamber No. 2 (see Table 13) for high-pressure testing.

Instrumentation arrangements for pressure and flow control in the high-pressure pulse-jet system are schematically illustrated in Fig. 10. The pneumatic controls and valves required have been ordered.

d. Future Work

Debugging of the ambient-pressure pulse jet and resonant manifold will continue. Design, manufacture, and procurement of items for the high-pressure test equipment will also continue, along with fabrication and installation of the high-pressure control panel and supply systems.

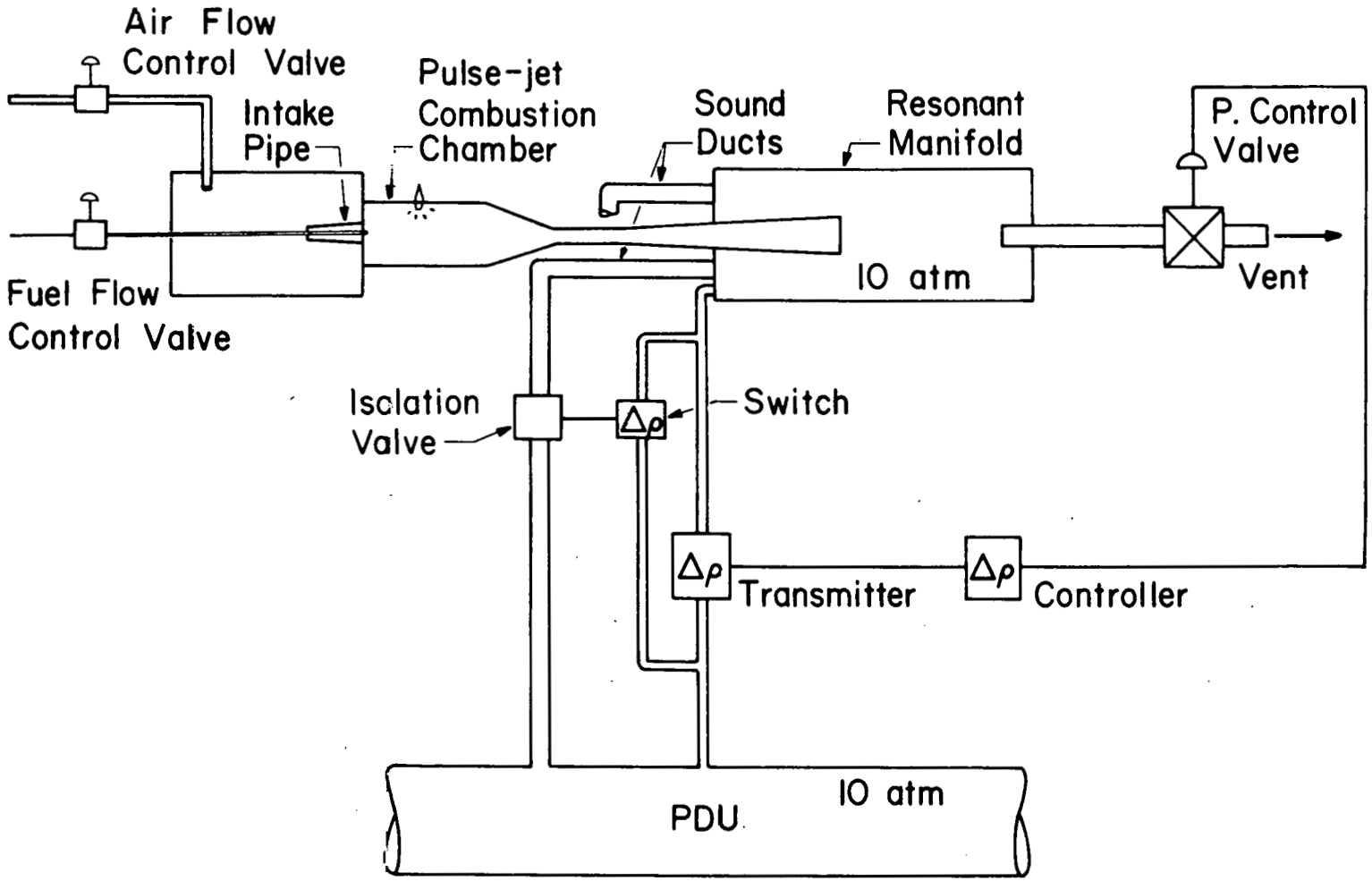

Fig. 10. Schematic Diagram of Pulse-Jet Phase II Instrumentation

2. TAN-JET Cyclone

After considerable delay, a controlled-vortex high-efficiency cyclone (TAN-JET) has been received from the Donaldson Company for testing and evaluation in the flue gas system of the ANL 15.2-cm-dia combustor (see ANL/CEN/FE-77-3 and ANL/CEN/FE-77-8). The cyclone will be extremely useful in testing of the granular-bed filter concept being evaluated at ANL and in evaluating the acoustic dust conditioning concept. Installation of the TAN-JET will require considerable modification to the existing flue-gas system. Piping diagrams and support structures for the cyclone have been prepared and are being prefabricated for installation where possible. When prefabricated items are completed and there is an appropriate break in the testing schedule of the combustor, installation of the cyclone will proceed.

3. Granular-Bed Filter

Initial testing of a granular fixed-bed filter in the flue gas system of the ANL 15.2-cm-dia combustor was recently completed. Results of the tests, which were performed to test the concept of using the limestone from the PFBC process as the granular-bed medium, were reported previously (see ANL/CEN/FE-77-8).

Currently, a conceptual design of a granular-bed filter for a 200-MWe demonstration facility is being made, based on the experimental results, to evaluate whether the basic concept of using limestone in the filter is feasible.

The basic assumptions for the conceptual design are given in Table 14. A simple mass balance based on the assumptions was made and is presented in Fig. 11. The mass balance indicates that ∿17.3 Mg/h of solids overflow from the combustor would be available for use in the granular-bed filter as the filtration medium. Based on a bulk density of 1370 kg/m^3 for the sulfated sorbent, ∿12.6 m^3/h of the sulfated sorbent would be available for use in the granular-bed filter.

Irrespective of the granular-bed filter design, a simple mass balance can be made on the filter to indicate maximum filter cross-sectional surface area as a function of granular-bed filter thickness and frequency of filter regeneration, *i.e.*, the number of times the granular bed would be changed per hour of operating time. The results of this analysis are shown in Fig. 12. At a given bed thickness, the maximum filter area possible decreases rapidly as the frequency of bed regeneration (cleaning) increases. At a bed thickness of 10 cm, for example, increasing the number of bed changes per hour from 0.5 to 3.0 decreases the maximum filter area possible from ∿255 m^2 to ∿42 m^2.

The material balance around the combustor also allows calculation of the volumetric flow rate which would have to be handled by the granular-bed filter. Thus, the linear velocity of the flue gas through the granular-bed filter can be calculated as a function of the filter surface area, the operating temperature, and the pressure. Figure 13 illustrates the results for a filter operated at 815°C.

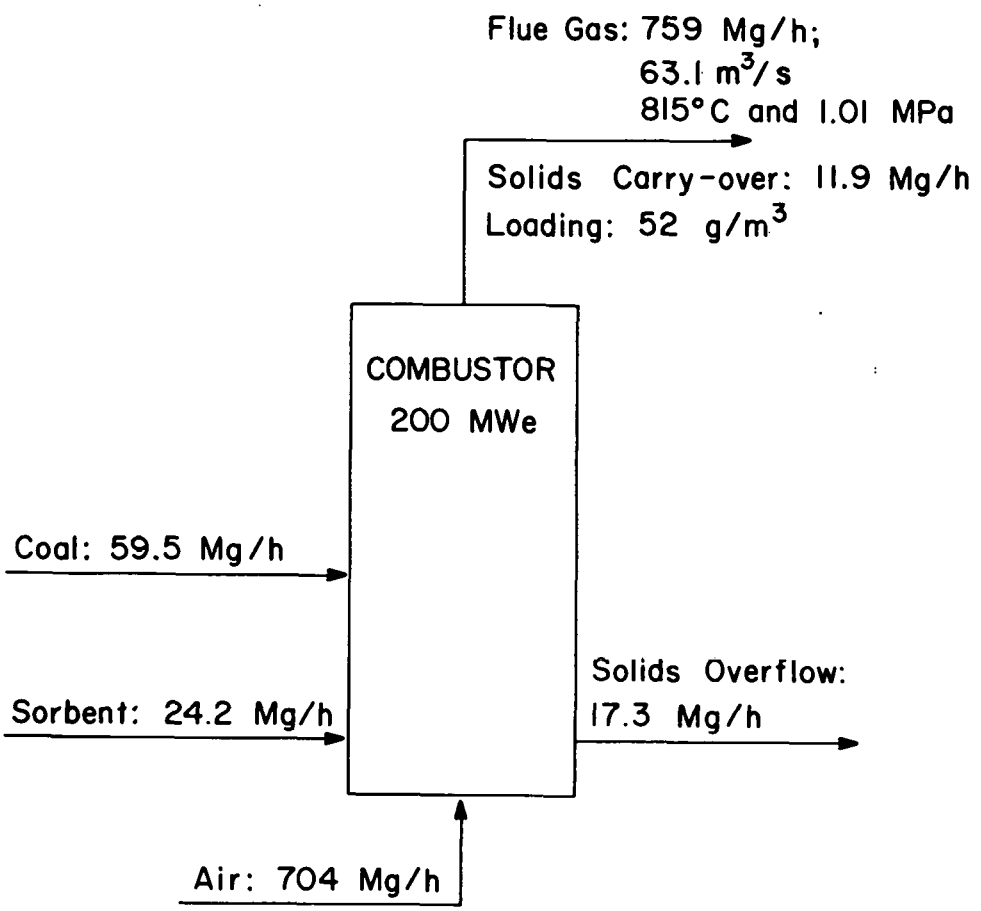

Fig. 11. Material Balance for 200-MWe Demonstration Plant Based on Assumptions in Table 14.

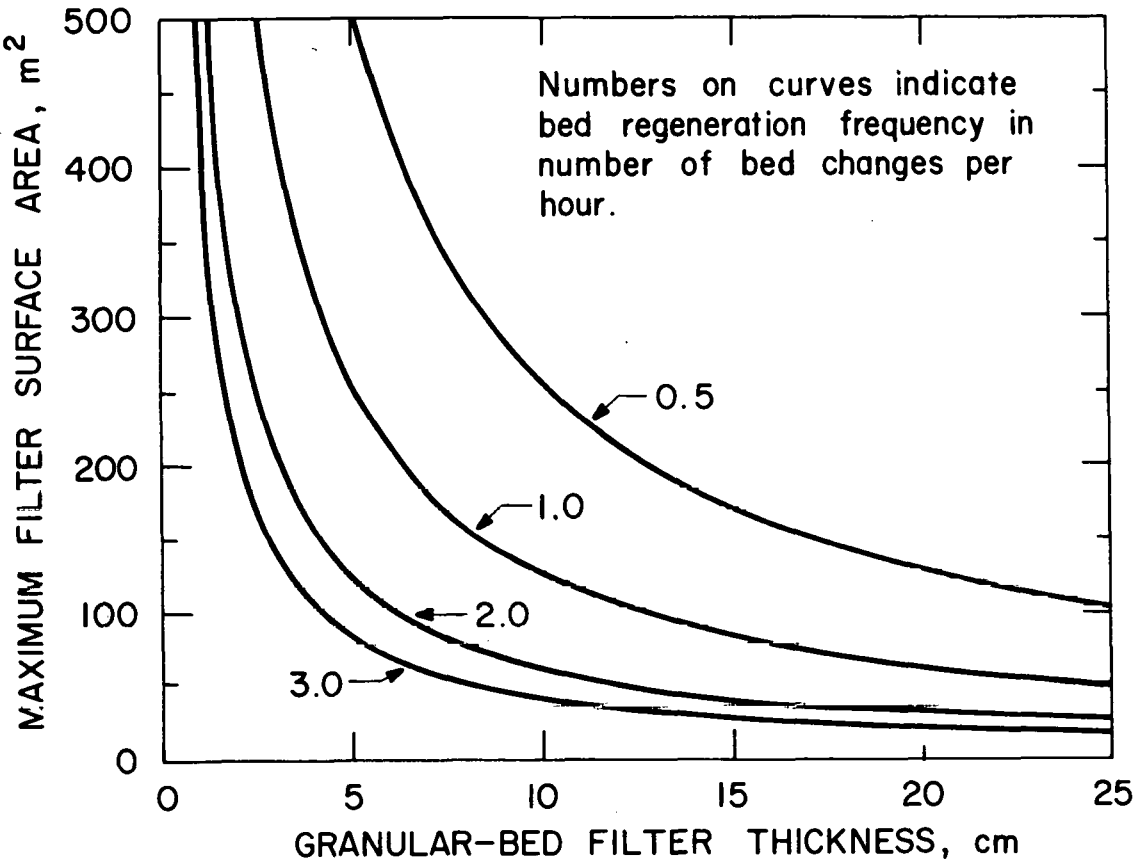

Fig. 12. Maximum Granular-Bed Filter Surface Area as a Function of Bed Depth and Bed Regeneration Frequency

The significant observation to be made from Fig. 13 is that to maintain a relatively low gas velocity through the filter, *i.e.*, 0.1 to 0.2 m/s, a total filter surface area between ∿160 m^2 and 630 m^2 is required, depending upon the system operating pressure. Referring back to Fig. 12, in order to design a granular-bed filter with 160 m^2 (the surface necessary to handle 63.1 m^3/s of gas at 815°C, 2.02 MPa, and a gas velocity of 0.2 m/s and a granular-bed filter thickness of 10 cm requires that the bed be replaced more often than once per hour.

The next step in the analysis will be to determine the initial pressure drop across the clean filter as a function of velocity, bed depth, pressure, and the rate of pressure drop increase across the bed as a function of velocity. The initial pressure drop across the clean bed can be estimated from the Ergun correlation, and the increase in pressure drop with time can be estimated from the experimental results reported previously.

Table 14. Assumptions used as a Basis for the Conceptual Design of a Granular-Bed Filter for a 200-MWe Demonstration Plant

Coal:	Sewickley coal with a heating value of 13,000 Btu/lb and containing 4.3% sulfur
Sorbent:	Tymochtee dolomite containing 20 wt % calcium, once-through operation
Excess Air:	20%
Ca/S Ratio	1.5
Cycle Efficiency:	40% (conversion of heating value in coal to electric power)
Bulk Density of Sulfated Sorbent:	1370 kg/m^3
Particle Carryover in the Flue Gas:	100% of coal ash plus 20% of sorbent

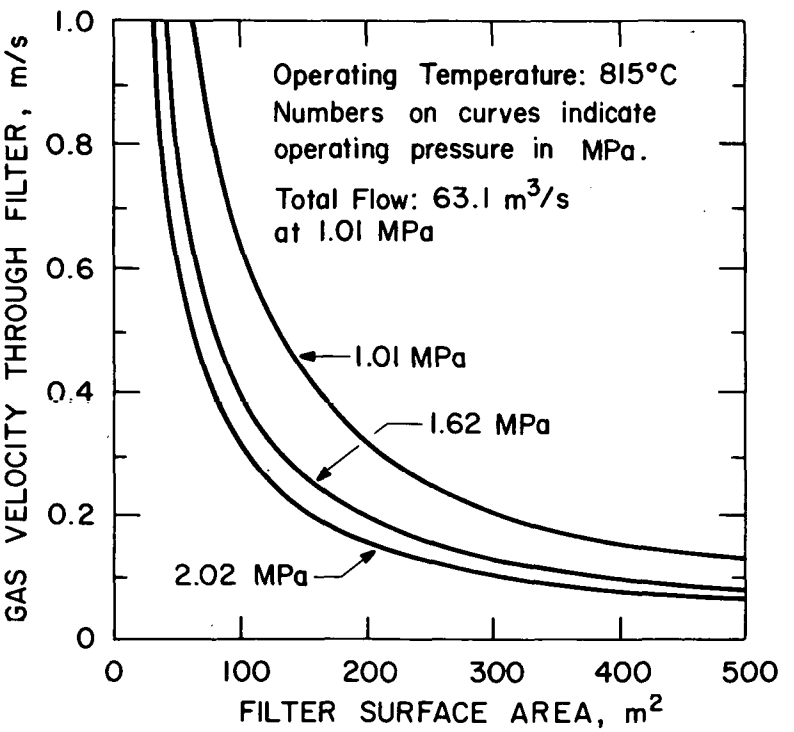

Fig. 13. Gas Velocity through Granular-Bed Filter as a Function of Filter Area and Operating Pressure

REFERENCES

1. D. L. Keairns *et al.*, Fluidized-Bed Combustion Process Evaluation, Phase II, Pressurized Fluidized-Bed Coal Combustion Development, EPA-650/2-75-027-C Westinghouse Research Laboratory, Pittsburgh, Pennsylvania (September 1975).

2. Methods of Analyzing and Testing Asland Slag, Methods of Analyzing and Testing Coal and Coke, Bulletin 638, p. 76, Bureau of Mines (1967).

3. J. Szekely, J. W. Evans, and H. Y. Sohn, Gas-Solid Reactions, Chapter 2, Academic Press, New York, 1976.

APPENDIX A

Limestone Designations and Sources

Limestone	Limestone Supplier	Location
ANL-4801	Midwest Aggregates Corp.	Fort Wayne, IN
ANL-4901	--	Monroe, WI
ANL-4902	Vulcan Materials	McCook Complex, IL
ANL-4903	Black Creek Limestone Co.	Black Creek, WI
ANL-5001	Harris Limestone Co.	Piedmont, MO
ANL-5101	E. E. Duff and Sons	Huntsville, OH
ANL-5102	Porter Limestone Co.	Rockton, IL
ANL-5201	Midwest Aggregates Corp.	Fort Wayne, IN
ANL-5202	Midwest Aggregates Corp.	Fort Wayne, IN
ANL-5203	Bullitt County Stone Co.	Shephardville, KY
ANL-5204	James River Limestone Co.	Buchanan, VA
ANL-5205	Mayville White Lime Works	Mayville, WI
ANL-5206	Mayville White Lime Works	Mayville, WI
ANL-5207	Quapaw Co.	Drumright, OK
ANL-5301	Chas. Pfizer Co.	Gibsonburg, OH
ANL-5302	Vulcan Materials Co.	Birmingham, AL
ANL-5303	May Stone and Sand	Fort Wayne, IN
ANL-5304	Vulcan Materials Co.	Parsons, TN
ANL-5401	Delta Mining Co.	Mill Creek, OK
ANL-5402	Raid Quarries (Medusa Aggregates)	Burlington, IA
ANL-5403	U. S. Steel Corp.	Chicago, IL
ANL-5501	Lime Products Corp.	Union, ME
ANL-5601	Kaiser Refractories	Salinas, CA
ANL-5602	G. & W. H. Corson, Inc.	Plymouth Meeting PA
ANL-5603	York Stone Co.	York, PA
ANL-6101	Jeffery Limestone Co.	Parma, MI
ANL-6301	Meshberger Stone, Inc.	Columbus, IN
ANL-6401	G. & W. H. Corson, Inc.	Plymouth Meeting, PA
ANL-6501	Meshberger Stone, Inc.	Columbus, IN
ANL-6701	Osmundson Bros.	Adams, MN
ANL-6702	Vulcan Materials Co.	Parsons, TN
ANL-7401	Fort Calhoun Limestone Co.	Fort Calhoun, NE

(contd)

APPENDIX A (Contd)

Limestone Designations and Sources

Limestone	Limestone Supplier	Location
ANL-8001	Greer Limestone Co.	Morgantown, WV
ANL-8101	Monmouth Stone Co.	Monmouth, IL
ANL-8301	Vulcan Materials Co.	Birmingham, AL
ANL-8701	--	--
ANL-8901	Hooper Brothers Quarry	Weeping Water, NE
ANL-8902	Vulcan Materials Co.	Parsons, TN
ANL-8903	Civil Bend Bethany Falls	Bethany, MO
ANL-9201	Georgia Marble Co.	Tate, GA
ANL-9401	Pete Lien and Sons	Rapid City, SD
ANL-9402	Lime Products Corp.	Union, ME
ANL-9501	Grove Lime Co.	Stephens City, VA
ANL-9502	American Aggregates	Indianapolis, IN
ANL-9503	Southern Materials	Ocala, FL
ANL-9504	Rose Equipment, Inc.	Weeping Waters, NE
ANL-9505	Midwest Minerals	Pittsburg, KS
ANL-9601	Columbia Quarry Co.	Valmeyer, IL
ANL-9602	Delta Mining Corp.	Mill Creek, OK
ANL-9603	G. & W. H. Corson, Inc.	Plymouth Meeting, PA
ANL-9701	Greer Limestone Co.	Morgantown, WV
ANL-9702	Hemphill Brothers	Seattle, WA
ANL-9703	Austin White Lime Co.	McNeil, TX
ANL-9704	Midwest Limestone Co.	Gilmore City, IA
ANL-9705	Western Materials Co.	Orleans, IN
ANL-9706	U. S. Steel Corp.	Chicago, IL
ANL-9801	Iowa Limestone Co.	Alden, IA
ANL-9802	Chem. Lime Inc.	Clifton, TX
ANL-9803	Rigsby and Barnard Quarry	Cave In Rock, IL
ANL-9901	Western Materials Co.	Orleans, IN
ANL-9902	Southern Materials	Ocala, FL
ANL-9903	Calcium Carbonate Co.	Fort Dodge, IA

APPENDIX B

Composition (wt %) of Limestones and Dolomites

Limestone	$CaCO_3$	$MgCO_3$	Fe_2O_3	Al_2O_3	SiO_2	Na_2O	K_2O
ANL-5801	48.7	40.2	0.66	1.81	7.0	0.09	0.38
ANL-4901	49.9	43.0	1.69	0.93	1.69	0.05	0.12
ANL-4902	49.7	43.8	0.43	0.87	5.71	0.03	0.30
ANL-4903	49.2	44.6	0.52	0.90	8.77	0.05	0.50
ANL-5001	50.4	43.0	0.37	0.98	3.52	0.34	0.10
Tymochtee (ANL-5101)	51.8	43.3	0.41	1.46	3.61	0.07	--
ANL-5102	51.2	43.4	0.62	0.43	1.2	0.05	0.19
ANL-5201	52.2	43.0	0.26	0.68	1.22	0.07	0.13
ANL-5202	52.7	42.0	0.34	0.87	1.60	0.11	0.15
ANL-5203	52.6	36.4	0.58	1.13	8.77	0.04	0.18
ANL-5204	52.9	45.8	0.25	0.04	0.54	0.04	0.01
ANL-5205	52.1	41.0	0.07	0.16	3.79	0.04	0.01
ANL-5206	52.7	42.2	0.13	0.25	1.14	0.05	0.02
ANL-5207	52.3	37.5	2.35	1.0	3.64	0.09	0.16
1337 (ANL-5301)	53.4	45.4	0.07	0.08	0.69	0.05	--
ANL-5302	53.9	44.9	0.16	0.43	1.35	0.03	0.07
ANL-5303	53.7	42.8	0.30	0.31	2.94	0.04	0.10
ANL-5304	53.5	3.7	2.33	0.73	36.12	0.16	0.41
ANL-5401	54.5	42.9	0.07	0.34	1.04	0.04	0.1
ANL-5402	54.9	27.3	2.73	1.10	10.14	0.08	0.43
ANL-5403	54.0	44.1	0.08	0.17	0.62	0.03	0.07
ANL-5501	55.6	43.3	0.23	0.18	2.97	0.03	0.03
Dolowhite (ANL-5601)	56.8	45.6	0.09	0.01	0.18	0.02	--
ANL-5602	56.6	43.8	0.33	0.18	1.05	0.03	0.09
ANL-5603	56.3	41.7	0.46	0.60	1.08	0.2	0.22
1351 (ANL-6101)	61.2	28.7	5.56	0.51	3.15	0.13	--
ANL-6301	63.2	32.6	0.39	0.28	2.54	0.04	0.05
ANL-6401	64.2	29.5	0.33	0.69	5.10	0.15	0.31
ANL-6501	65.9	31.5	0.38	0.28	2.08	0.04	0.05
ANL-6701	67.3	31.5	0.37	0.22	1.25	0.04	0.15
ANL-6702	67.5	0.91	0.08	0.18	30.22	0.08	0.13
ANL-7401	74.7	10.2	1.07	1.82	11.2	0.19	0.36
Greer (ANL-8001)	80.4	3.5	1.24	3.18	10.34	0.23	--
1360 (ANL-8101)	81.6	11.6	0.86	0.19	1.86	0.10	--
ANL-8301	83.9	13.4	0.14	0.42	1.24	0.02	0.02
Chaney (ANL-8701)	87.0	1.2	3.4	2.0	7.1	<0.1	--
1343 (ANL-8901)	89.8	2.2	0.66	1.04	4.0	--	--
ANL-8902	89.6	3.02	0.37	0.79	5.06	0.03	0.29
ANL-8903	89.3	1.21	0.98	0.83	5.5	0.12	0.22
1336 (ANL-9201)	92.6	5.3	0.2	0.42	1.26	0.10	--
ANL-9401	94.1	1.0	0.35	0.51	3.18	0.05	0.10
ANL-9402	94.7	0.87	0.14	0.23	0.63	0.02	0.02
Grove (ANL-9501)	95.3	1.3	0.09	0.25	0.77	0.03	--
ANL-9502	95.6	3.36	0.05	0.11	0.42	0.02	0.04
ANL-9503	95.5	0.76	0.05	0.13	0.15	0.02	<0.01
ANL-9504	95.8	0.58	0.30	0.36	2.71	0.05	0.13
ANL-9505	95.1	3.47	0.90	0.29	0.70	0.04	0.03
2203 (ANL-9601)	96.5	3.3	0.17	<0.01	0.20	0.05	0.01

(Contd)

APPENDIX B (Contd)

Composition (wt %) of Limestones and Dolomites

Limestone	$CaCO_3$	$MgCO_3$	Fe_2O_3	Al_2O_3	SiO_2	Na_2O	K_2O
ANL-9602	96.2	0.43	0.12	0.21	1.19	0.03	0.01
ANL-9603	96.4	1.56	0.10	0.30	0.70	0.05	0.11
Germany Valley (ANL-9701)	97.8	0.6	0.10	1.8	0.2	0.25	--
ANL-9702	97.5	0.68	0.05	0.05	0.21	0.01	0.01
ANL-9703	97.6	0.58	0.19	0.50	1.08	0.03	0.17
ANL-9704	97.8	0.34	0.30	0.05	0.15	0.04	0.02
ANL-9705	97.3	0.53	0.17	0.35	0.20	0.05	0.01
ANL-9706	97.3	0.98	0.08	0.06	0.23	0.03	0.01
ANL-9801	98.3	0.6	0.15	0.16	0.20	0.04	0.20
ANL-9802	98.2	0.47	0.18	0.10	0.29	0.04	0.01
ANL-9803	98.0	1.26	0.07	0.14	1.47	0.02	0.02
ANL-9901	99.1	0.60	0.05	0.06	0.17	<0.013	<0.01
ANL-9902	99.1	0.38	0.05	0.04	0.13	0.04	0.01
ANL-9903	99.8	0.53	0.02	0.16	0.24	0.20	0.01

APPENDIX C. DEVELOPMENT AND APPLICATION OF A LASER SPECTROSCOPY SYSTEM FOR FBC GAS SPECIES MEASUREMENT: SYSTEM CONCEPTS EVALUATION

Prepared for:

ARGONNE NATIONAL LABORATORY
Argonne, Illinois 60439

Contract No. 31-109-38-4107

SPECTRON DEVELOPMENT LABORATORIES INC.

3303 Harbor Boulevard, Suite G-3
Costa Mesa, California 92626 (714) 549-8477

SUMMARY

The first part analyzes the problem to which the bulk of this and subsequent reports is primarily addressed. Some general phenomenology of the hot corrosion process caused by sulfate deposition is outlined and the measurement problems defined. Various physical phenomena are considered for their potential in making the required measurements. Others are considered, not for their usefulness, but for the degree to which they may obscure or render in error those in the former category. Many techniques which appear to be superficially attractive may be rejected for simple and unambiguous reasons - others merit further analysis and are shown here to be worthy of more detailed considerations.

TABLE OF CONTENTS

LIST OF FIGURES

LIST OF TABLES

1.0 INTRODUCTION

1.1 Background

There is very considerable interest in generating electricity from coal whose quality or sulfur content needs special combustion facilities to meet pollution requirements. Fluidized bed combustors with additives which prevent excessive emission of oxides of sulfur are being investigated, and to raise system efficiency combined cycle systems are under active examination. The major particulates are removed from the hot gas stream by cyclones and granular bed filters prior to impingement on the first stage of a gas turbine. The higher the turbine inlet temperature, in general, the more energy may be extracted and the more efficient the total system may be. There are, of course, limits on top temperature of turbine materials and it has become usual to arrange to cool the blade surfaces by injection of a cooler medium. The transpiration, injection or film cooling guarantees that the blade will be below the temperature of the gas stream and although this improves both efficiency, because a higher turbine inlet temperature is permitted, and blade life, from thermal considerations, there is a tendency for the less volatile species in the efflux of the coal burner to condense on the blade. Particularly prone to such condensation are the sulfates of alkali metals present both in the original coal and to a comparable extent in the dolomite added to suppress sulfur emission.

It appears from published data that hot corrosion of many turbine materials is initiated by a deposited layer of liquid sulfates of sodium and/or potassium. A mixture of these may melt at a lower temperature than either pure material, and indeed the presence of Ca or Mg sulfates may also alter the tendency to form a liquid layer.

It appears that if a thin layer of a liquid sulfate is present on the surface of a nickel-based alloy, where there is an excess of oxygen above the sulfate layer, that certain transport mechanisms operate. The partial pressure of oxygen at the base of the liquid layer causes a reaction with local surface NiO to form an unstable "nickelate" ion [NiO_2^{2-}] which migrates to the surface of the layer removing nickel. Residual sulfur at the base migrates into the nickel permitting the oxygen imbalance to be maintained. This sulfidation corrosion then proceeds to remove nickel at a high rate, the constant amount of sulfur migrating into surface layers of corrosion pits and the oxygen being supplied continuously from the surface. The Na_2SO_4 plays the part of a carrier medium in which the undesirable reactions may proceed, but it is not consumed. The corrosion therefore is an unstable "runaway" process for which prevention of the existence of a layer of liquid sulfate is much more effective than relying on methods for its removal. A detailed study of these mechanisms[1] is available.

It appears that although erosion and accretion fouling may be dependent upon gas borne particulates, the main source of hot corrosion initiators is direct condensation on the metal from the vapor phase. This is especially likely to occur on cooled elements such as the turbine blades. Unless there is significant presence of molybdenum oxide[2] it appears that liquid sulfate condensation (leading to sulfidation) is the dominant initiator of corrosion and hence is that property which must be monitored and controlled to reduce or prevent serious metal attack. The dominance of this mechanism is supported[3]

by the presence of corrosion after only a brief excursion into a Na_2SO_4 deposition regime.

From this the control function becomes such as to prevent any deposition, however transient, from occurring. Once any Na_2SO_4 has condensed, the damage is done and corrosion will continue catastrophically unless the sulfate layer either completely solidifies or is removed. Removal mechanisms for liquid sulfate are discussed in Reference 6. Condensation on upstream particles or cooler structures may protect the turbine blades, but is unlikely or undesirable: it is certainly not a long term solution in a continuously operating facility. Avoidance of Na_2SO_4 presence at concentrations above the deposition threshold for the blade temperature is a satisfactory preventive. It further appears that direct deposition as a solid, provided that it never reaches fusion temperature, is also a cure. It may not always be possible nor convenient to operate the turbine blades below the minimum melting temperature of any possible eutectic of deposited species.

Many references[4-9] introduce the somewhat complex high temperature chemistry and physics of the efflux from a fluidzied bed combustor. Other work has been directed towards the monitoring of emissions[10] and their control.[4-11] Non-intrusive monitoring is currently available commercially using various techniques for the pollutants which are more normally considered to be environmentally deleterious, *e.g.*, NO_x, SO_2, particulates, etc. The problem of nonintrusive monitoring of alkali metals and their compounds for corrosion avoidance is less well studied and certainly more difficult.

There are two classes of candidate techniques for trace species monitoring: (a) the analysis of an extracted sample and (b) the nonintrusive observation of a parameter quantitatively changed by the presence of the species of interest.

A discussion of class (a) is not appropriate to this report as it is being adequately pursued elsewhere. The consideration of class (b) is open-ended in that it should explore all techniques which might become economically feasible and offer advantages over analysis of an extracted sample with respect to process monitoring and control.

1.2 Environment and Constraints

The flue gases in a coal fired FBC would be at about 850°C (1123 K) and about 10^3 kPa (c. 10 atmospheres)[12] prior to entry into the combined cycle turbine. At this point the flue gases will have been through probably two cyclone separators and a granular bed filter which will have removed most of the particulates especially those in the larger size ranges, above a few μm (say). There may be particles below these sizes, and possibly even a few rogues which escape the clean-up process. The gases will contain a large number of residual molecules derived from contaminants in the original, fairly low and variable grade coal, and various sorbents added to minimize emission of sulfur oxides. The pipe which carries the flue gases in the facility in question for this contract has a typical diameter of 0.1 m and may be modified to accept windows, transparent to various sections of the electromagnetic spectrum. It is anticipated that the windows could be prevented from changing their transmission properties with time by one of a number of techniques widely used in those industries where such engineering arts are required, *e.g.*,

heating, cooling, purging, washing, etc. as appropriate. In this case we might suggest heating, an apparently curious choice until the other constraints of neither addition to nor subtraction from the test flow are considered. Cooling the window, often a popular method of protecting the window would here lead to condensation and immediate loss of transmission.

Many good techniques of analysis of trace species in gases are here precluded by the requirements not to extract a sample of the gas; such methods are the subject of other current studies which themselves offer great promise once the price of sample extraction is paid.

The gases may thus be observed via one, or two opposed, window(s) and although flowing past at some speed may be assumed to be in complete chemical and thermodynamic equilibrium. Thus the time scale of concentration change is characterized by response times of the FBC over bed chemical make up to changes in combusting materials. This will almost certainly be of order ms and larger, probably up to hours as feedstock chemistry varies. Particle loading may vary very rapidly, having consequences of varying seriousness depending upon the monitor method which we choose to use.

1.3 The Problem

The purpose for which this contract was established is seen to be that of monitoring the gaseous concentration of alkali metal sulfates with particular regard to detecting the point at which there may exist, for whatever reason, a layer of liquid sulfate upon the surfaces of turbine blades. Such a thin layer in the liquid phase only will lead to severe metal attack and removal of most probably the nickel, of most suitable turbine blade alloys. This does not, of course, apply to ceramic blades which may gain popularity in the future.

The accurate monitoring of this condensation point may ultimately be used as a control parameter for bed additive chemistry to avoid the corrosion condition. The quintessence of control is to avoid the deposition of any sulfate. The corrosion mechanism appears to use sulfate as a catalytic initiator whereby a local medium is provided which prevents nickel passification and provides oxygen transport and nickel oxide removal as an unstable transient "nickelate". There are other suggested mechanisms but this is adequate to provide necessary and sufficient condition to prevent deposition of sulfate.

The presence of sodium and sulfur compounds in the fuel and pollution control additives makes it certain that if the emitted quantities of these are high enough the sodium species found in the gas phase will be sodium sulfate, chloride and oxide/hydroxide with sundry dimers. An equilibrium distribution is shown in Reference 6 and reproduced here as Figure C-1. An equilibrium pressure map from the same reference is included as Figure C-2, and a product distribution map for varying fuel air ratio from Reference 9 as Figure C-3. There is a wealth of technical data in the literature but in most cases the emphasis has been on theoretical predictions from the basis of chemical thermodynamics. Measurements have proved to be difficult in these harsh engineering environments. What measurements do exist indicate that the theoretical assumptions have been quite adequate as far as they have gone but a complete characterization of what is going on in combined cycle demonstrator and proposed full scale installations is yet to be detailed.

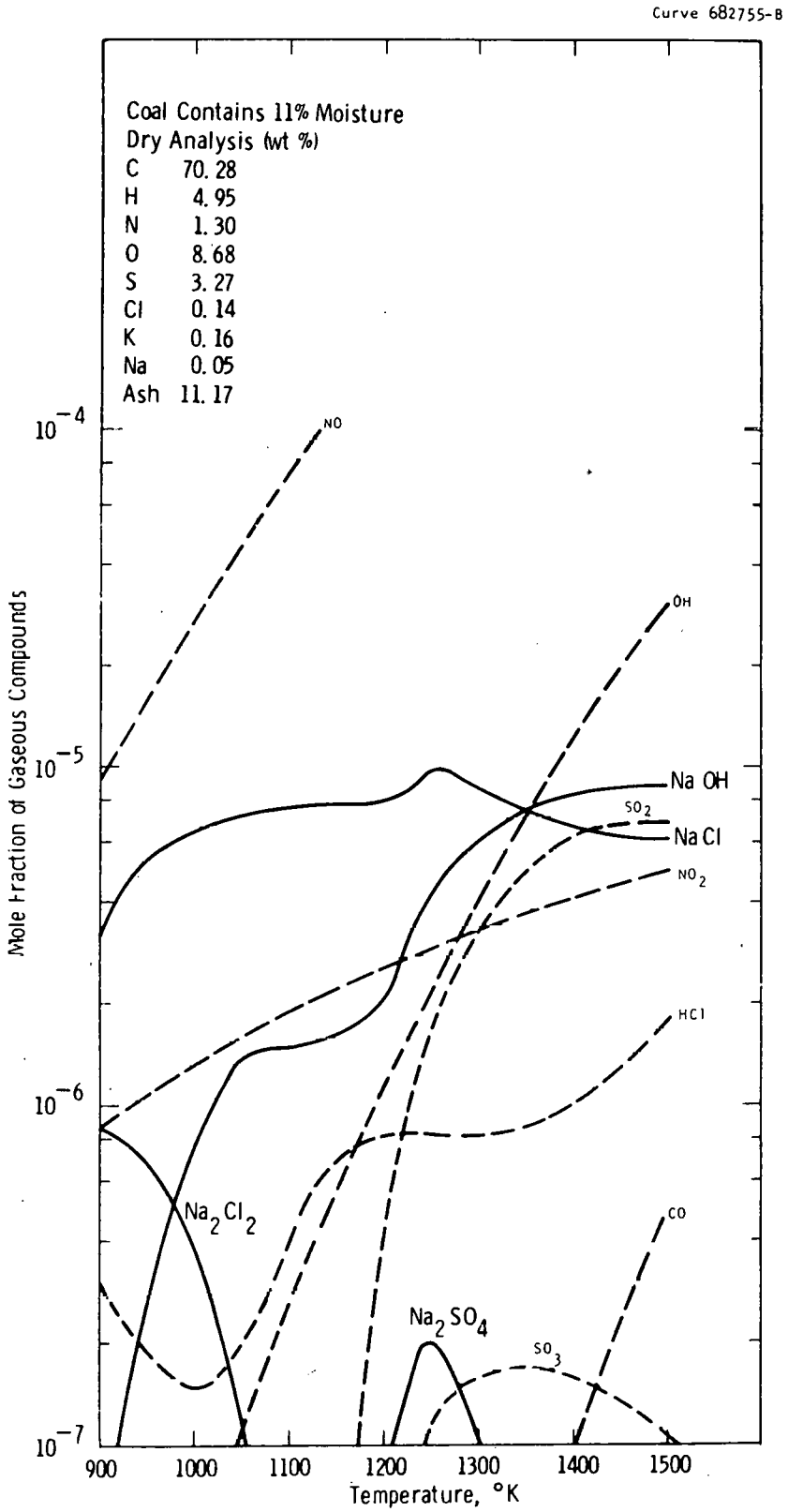

Fig. C-1. Equilibrium Product Distribution in Fluidized Bed Combustion at One Atmosphere (from Ref. 6)

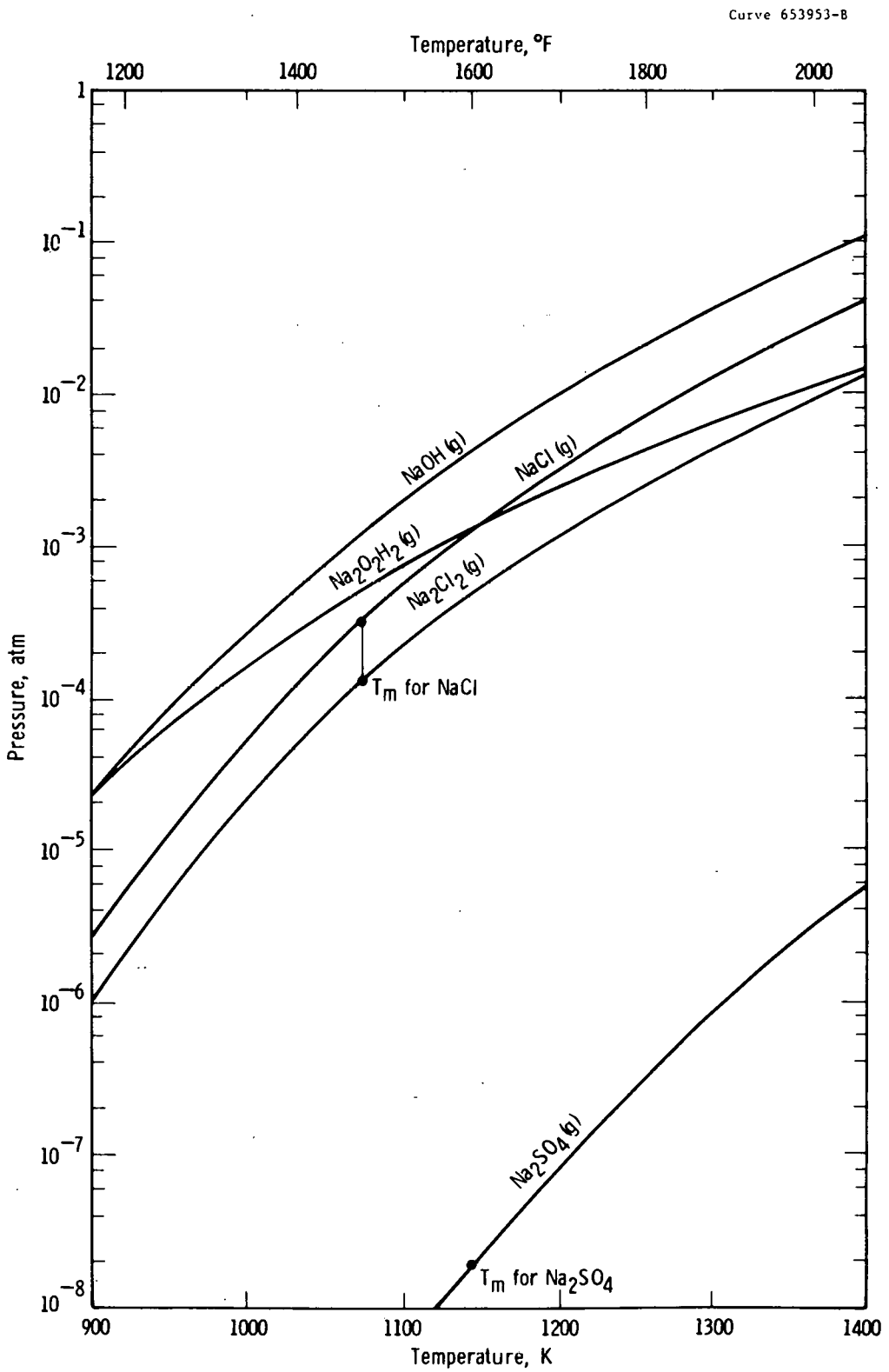

Fig. C-2. Equilibrium Pressures for Sodium Species Over NaOH, NaCl and Na_2SO_4 Condensed Phases (from Ref. 6)

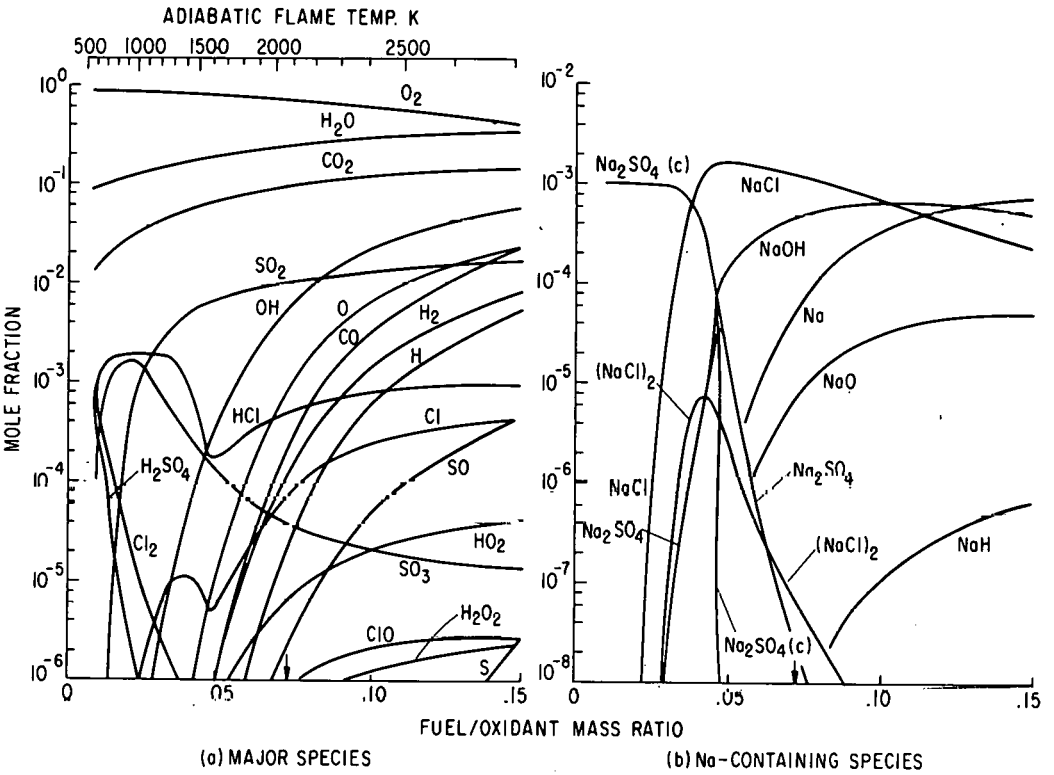

Fig. C-3. Equilibrium Chemical Composition for NaCl-SO_2-doped CH_4-O_2 Flame. Arrows Indicate Fuel/Oxidant Mass Ratio of Flame Used (from Ref. 9)

The main controlling parameter for deposition of sodium sulfate, which appears in this Argonne application to dominate the potassium effects, is, not surprisingly, the concentration of Na_2SO_4 in the gas phase. There seems no clear mechanism for transferring sulfates from particulates to blade surfaces except via the vapor phase so for the purposes of this initial exercise the particles are regarded only as a source of error or inconvenience in the assessment of gaseous concentrations, and are discussed as such. We may justify this further by noting that since the blades are cooler than the gas stream, if there exists any Na_2SO_4 either as liquid or solid on the particles it will be in equilibrium with the gaseous Na_2SO_4, and hence evaporate or sublime to be deposited on cooler surfaces. The probability of this process will be accessible via measurement of gas phase concentrations.

The presence of sodium sulfate as an undissociated molecule in these environmental conditions is a consequence of its great stability. Knowing other properties, such as temperature, it may be possible to infer its concentration by measurement of more easily qualified molecules known to be in equilibrium with it, *e.g.*, NaCl. It is unfortunate that at these temperatures and pressures the equilibrium concentration of free sodium is vestigial; so many orders below the other constituents that even with single atom detection methods the level would be too low for accurate assay.

The required limits of measurement of alkali sulfate for this contract have been stated to be 0.1 mg m^{-3} to 100 mg m^{-3} with precision of 0.1 mg m^{-3} to 5 mg m^{-3} respectively as discussed in Reference 12 and it is certain that the concentration of Na_2SO_4 at which condensation begins lies somewhere in this range. Whether it will condense as a solid or liquid depends on blade temperature and other constituents which may lower the melting point.

There are three classes of method whereby sodium sulfate may be measured without extracting a sample.

(1) Direct measurement of some molecular property,

(2) Inference from a direct measurement of another species in assumed equilibrium with it,

(3) Inducement of some change in the sulfate or an equilibrial species to enhance the possibility of measurement.

A list of possible candidates is offered in the next section.

1.4 Possible Techniques or Related Phenomena

The analysis of trace species where no sample may be withdrawn must rely on acquisition of information/energy from within the remote region by a transducer. This information must indicate concentration and type of material. In solids and liquids it is possible to envisage several mechanisms, but in gases the only serious contender for such an information channel appears to be electromagnetic radiation. The radiation may be spontaneously emitted from the test region or it may be produced elsewhere and be modified in intensity, frequency or polarization by constituents of the test space.

Different regions of the electromagnetic spectrum indicate different properties of atomic species and molecules. The gamma and x-ray regions are indicative of nuclear properties, the ulta-violet and visible indicate the electronic properties of atoms and molecules, the near and far infrared show vibrational and rotational properties of molecules and into the microwave region electron spin and nuclear magnetic resonance phenomena occur. In principle most of these types of radiation may be considered candidates for species analysis. Each will be briefly discussed, and is illustrated schematically in Figure C-4.

Requirements for operating a diagnostic technique are appropriate radiation detectors, filters and other components and in the absorption and scattering mode suitable sources. The various phenomena are considered as possible candidates in the light of the problem as it is currently posed.

1.4.1 Techniques for Trace Analysis

Possible methods based on remote sensing of electromagnetic radiation created in, or modified by, the test gas may include the following. All are based upon frequency resolution appropriate to some atomic or molecular structure and rely on scatter or absorption of incident radiation or characterization of natural emission.

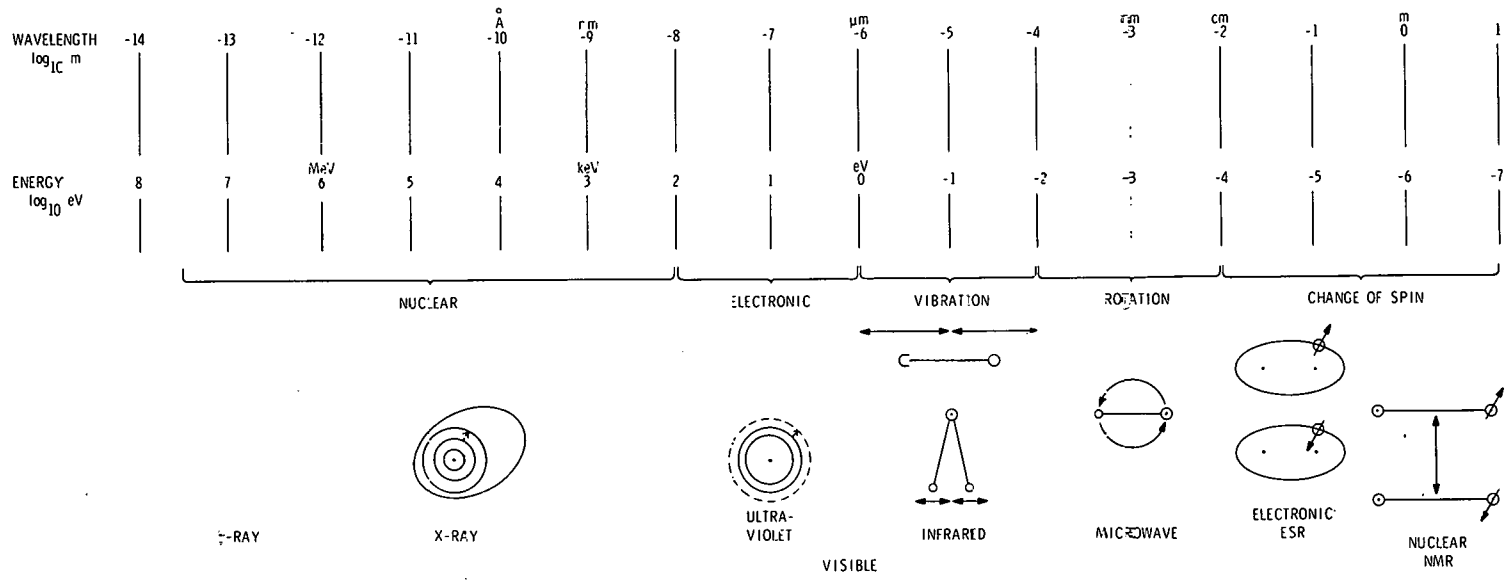

Fig. C-4. Characteristic Phenomena.

Nuclear Transitions	10^3 - 10^8 eV or 10^{-4} Å - 10 nm
Atomic and Molecular Electronic	50 nm - 3 μm
Molecular Vibration/Rotation	1 μm - 50 μm
Molecular Rotation	50 μm - 500 μm
Electronic Spin Resonance	10 mm - 10 cm
Nuclear Magnetic Resonance	10 cm - 10 m

- Nuclear Magnetic Resonance
- X- and gamma ray absorption
- Molecular electronic transitions
- Molecular vibration/rotation transitions
- Dissociation and atomic transitions in Na

The major problems with each of these methods are the low concentrations to be measured and the hostile environment in which these measurements must be made. We will consider the possibility and subsequently practicality of different methods.

All the above may be ligitimately considered as spectroscopy. It seems that the first two, although widely used have not been applied to such a high density hot engineering situation and the development which would be required would be a project of many years, fraught with uncertainties and low probability of success. That is not to say that they must be rejected forever although neither may be adequate at the very low concentrations of interest.

There follows a list of phenomena which are currently used for chemical analysis of trace constituents without modifying the sample. These must be rejected for at least one and often more of the following reasons.

(a) The phenomenon is only applicable to the molecular species in the solid, or sometimes liquid form.

(b) The technique requires a relatively high concentration of the species to be identified, compared with the trace levels here.

(c) Either the physical environment in the test space or in the proximity of the harsh operating condition precludes the use of the phenomena without extensive additional research and technology, or sometimes at all.

It seems useful to list all techniques which we have considered now in case their non-applicability is seen to be changed by developments on a wide front of process instrumentation. At the moment none of these techniques could come into the class of presently useful techniques for this problem and it is that function which is required as a result of this contract.

In each of these cases there may be other reasons but the ones presented are sufficient to reject the methods for the present purposes. Please see Table C-1.

In the spectrum presented as Figure C-4 we have rejected phenomena based on the extremely short and extremely long wavelengths. It is sensible to define bounds of wavelength beyond which it is not feasible to pursue the techniques. The very short x- and γ-ray are rejected at low concentration at least because any observation scheme would have great difficulty discriminating against the cosmic ray background as "good" events would be rare. Also

Table C-1.

Immediately Rejected Techniques		Reason
NMR	Nuclear Magnetic Resonance	(b,c)
PAC	Perturbed Angular Correlation	(a)
IMPACT	Implantation Perturbed Angular Correlation	(a)
EPR	Electron Paramagnetic Resonance	(c)
ENDOR	Electron Nuclear Double Resonance	(b,c)
LEED	Low Energy Electron Diffraction	(a,c)
SHEEP	Scanning High Energy Electron Diffraction	(a,c)
FIM	Field Ion Microscopy	(c)
	Mössbauer Spectroscopy	(a)
	x-ray and γ-ray Spectroscopy	(b)
	Electron Spin Resonance	(b,c)

neutron bombardment sources would have to be very intense and utterly intractable for these purposes. Difficulties of signal to noise problems are to be expected at the long wavelength also as specific photon energy is very low compared to the thermal background.

Of most appeal is the range of electromagnectic wavelengths in the near ultraviolet, visible, and infrared. These have been grouped as "optional" wavelengths and it is in these regions that we next explore phenomena.

1.4.2 Optical Phenomena

The use of visible radiation as the probing wavelength range offers many advantages. Sources are readily available, detectors may be essentially quantum limited and there are several window materials available. There exists wide experience of diagnostic analysis within and near the visible spectrum applied to hostile environments.

Techniques may be elastic or inelastic, the latter category capable of expansion to include more complex atomic and molecular interactions. In general the elastic scattering phenomena are not specific.[13]

1.4.2.1 Inelastic Techniques

These correspond typically to the center three sections on Figure C-4. The stereochemistry of sodium sulfate suggests a central sulfur atom surrounded by a tetrahedral array of oxygen atoms between two opposed pairs of which the sodium atoms are situated. This is a compact and highly stable complicated structure whose electronic spectrum is exceedingly complex and whose vibration and rotation spectral levels are elaborate and smeared into a quasi-continuum, at least as far as currently available data would suggest. Figure C-5 shows typical spectra obtained by different methods but none, unfortunately, referring to the required gaseous state. There is no resolution of any detailed structure in the absorption bands, nor would any be expected in this physical state. In low pressure gaseous form this structure might be resolvable (although we have found no reference to such nor any relevant published data) but to a large extent this may be lost in the high pressure and high temperature environment here. Even though the partial pressure of sodium sulfate is very low the doppler and collisional broadening due to the high temperature and pressure would contribute to mask any detailed structure.

Most of the techniques listed in this section require the existence of a suitable spectral line. By "suitable" we mean one which exhibits the properties to which the chosen method is sensitive, the existence of suitable detectors at that wavelength and in several cases the availability of appropriately narrow and/or powerful radiation sources and other components. In general none of these constraints is trivial.

Again the earlier constraints seem to eliminate some features but it is more proper here to expand upon some of the techniques for present information and so that this may be used as a source and reference document as further technology becomes available.

Linear inelastic scattering phenomena typically involve an energy change to the scattered photon and an equivalent energy and momentum conservation change to the atomic or molecular system. The latter may include an energy change in the electronic, vibrational or rotational levels and is rendered specific to the system by the quantum selection rules obtaining. The magnitude of the transitional energies is most for electronic, less for vibration and usually small for rotation but since there is coupling between the various levels a large number of wavelength shifts is possible. The classification of these processes is not always as clearly expressed as might be helpful and this will be a very brief outline based on data from a number of sources.

(a) Raman: Inelastic processes occurring within times of typically 10^{-12} s show a wavelength shift characteristic of the atom of molecule involved in the interaction. Cross sections are usually of order 10^{-30} cm^2 per atomic or molecular system, very much smaller than any reasonable physical size which might be associated. This difference may be simply explained by noting that the incident photon frequency is far away from a system resonance. It is apparent that Raman experiments may be performed with incident light over a wide range of wavelengths where sufficient optical power is available. The scattered spectrum, of which a typical example is taken from Reference 15 as Figure C-6, shows features characteristic of several parameters. The displacement in wavelength of the vibration line is an indicator of the scattering species, the intensity of the scattered light is an

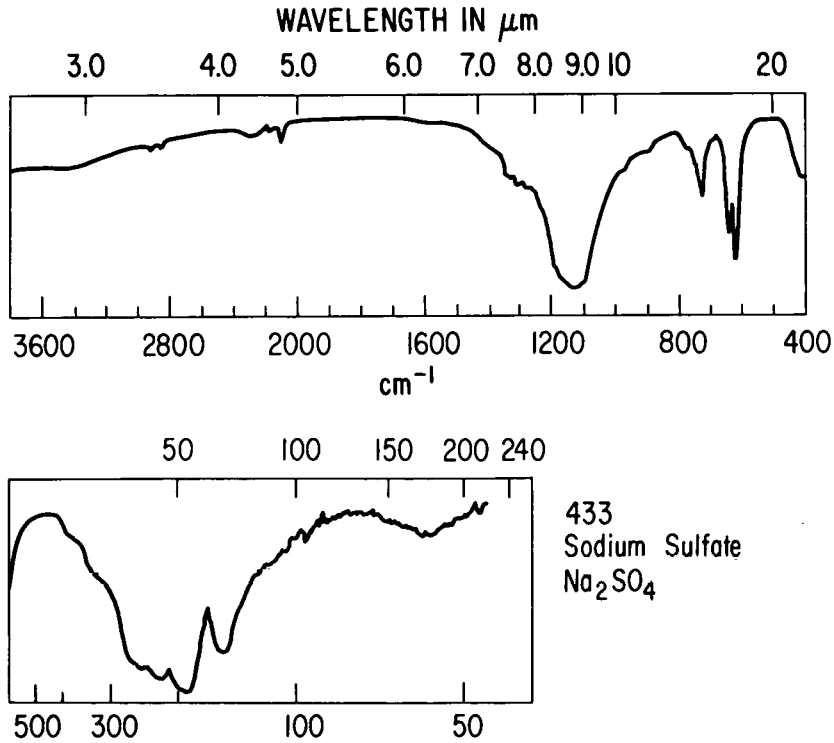

Fig. C-5. Published Spectra for Sodium Sulfate. Reproduced by permission of Academic Press. From R. Nyquist and R. O. Kagel, Infrared Spectra of Inorganic Compounds, 1971.

indication of the concentration of that species. The temperature may be determined from the ratio of the intensities of vibration lines at higher and lower wavelength than the exciting frequency (Stokes to Anti-Stokes ratio) or from the rotational structure of the line shifted to longer wavelength. This latter is larger than the Anti-Stokes line because at temperatures less than 1000 K to 2000 K the thermal excitation energy is such that the probability of an increase in photon energy at collision is still significantly lower than the probability of a decrease. Statements about temperature must be made with caution unless it is possible to assume that translational, vibrational and rotational temperatures have reached equilibrium. The vibrational lines are broadened by the presence of rotational splitting which may only be sensibly observed under conditions of high resolution, high scattered light intensities and great care. The low cross sections combined with low species concentration make it possible to measure the levels only of constituents which are present at 1 part in 1000 or more with the presently existing technology. This conclusion has been verified by a number of recent workers in this field. This is obviously sufficient disadvantage to prevent its direct use for measurements of trace quantities of sodium sulfate, even provided that the details of the Raman spectrum were obtained and were subsequently found suitable for this application.

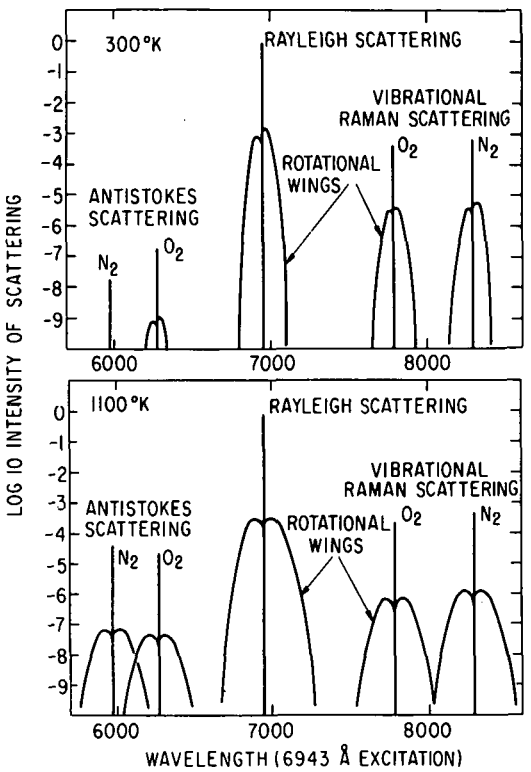

Fig. C-6. Raman and Rayleigh Scattering for Air, Drawn Roughly to scale, at Room Temperature and 1100° K. To the scale of this drawing, ground state and upper state fundamental vibrational Raman bands are not distinguishable. Reproduced by permission of Plenum Publishing Co. from M. Lapp and C. Penney, Laser Raman Gas Diagnostics, 1974.

(b) Near Resonant Raman: The cross-section of a Raman scattering process may be enhanced by the proximity of the illuminating radiation to a resonant transition. For most substances the transition chosen would be electronic (possibly vibrational) and the section enhancement could be up to 10^6. This is not realized in general because the position of resonances is not compatible with existing suitable light sources and detectors such that the theoretical advantage is partially or wholly lost in the experimental realization. In the case of sodium sulfate the electronic transitions are very complex and not conveniently within the range of currently available ulta-violet lasers and the vibrational bands in the infrared have much reduced scattering efficiency, reducing the apparent gain. One significant property of near-resonant Raman is the freedom from quenching because the 'lifetime' of the event is $\sim 10^{-12}$ s, shorter than typical collision times, and this property may make this technique attractive in many cases. It is unfortunate that the advantage it would offer in this case is not realizable for these other reasons.

(c) Resonant Raman or Fluorescence: Some distinguish between these on the basis of relative linewidth but we shall use both the terms for stimulation of a particular transition by a resonant wavelength. The cross-sections for this process are enormous compared with other Raman processes as would be expected for resonance phenomena. A rider to this increase is the dilation of the interaction time which may be four or more orders of magnitude longer. In an ideal case, for low molecular density this would have no serious diagnostic consequences and measurements could be made either of scattered radiation with the attendant spectral properties or of the absorption coefficient

in the narrow stimulation band. The problems arise out of the probable large number of molecular collisions which are to occur before the re-emission of radiation. This collisional quenching may cause the incident radiation to be dissipated as kinetic energy, dissociation, chemical change or change of internal energy, in none of which cases the radiation, if any, is unambiguously associated with the specific classification of the molecule. It is theoretically possible to allow for the quenching effects by measuring all the molecular properties of all species present and allowing for the changes in radiation brought about by their simultaneous presence. In the case of high pressure combustion efflux this is quite inconceivably complex.

There exists the technique of saturation fluorescence whereby there is an equilibrium established between the excitation rate and the de-energization by all mechanisms including radiation but this is not likely to avail to produce measurable signals in the case of sodium sulfate at high pressures and in low concentrations.

(d) Resonant Absorption: Because of dominant quenching effects in high pressure gases it is not feasible to use the light scattered or, more accurately, absorbed and re-emitted with or without a different frequency as an indication of trace constituent species concentration. It is however feasible to measure the attenuation of a line at which the trace species has a high resonant absorption coefficient, assuming that there are no interfering effects in that frequency band. In the case of sodium (or related alkali metal) sulfates there are no resonant absorption lines in the visible spectrum. The electronic transition lines are smeared into bands in the ultraviolet because of the energy properties and high complexity of the system and the thermodynamic conditions of the sample. Not only are there no suitable ultraviolet sources of suitably narrow width, there is no guarantee of specificity in that band of the combustion product system under examination here. There are absorption bands in the infrared, the most likely candidate being the 950-1200 cm^{-1} band (see Reference 16 and Figure 5). Bands further into the infrared begin to pose problems more serious to the engineering of a measurement system based on these phenomena.

There are, however, problems associated with this. Most alkali metal sulfates have bands in this region as may other trace constituents. Data are not currently available at the resolution required to decide unequivocally whether this technique would be applicable from a phenomenological viewpoint. The feasibility on engineering grounds is another discussion but less likely to prevent the technique from being usable even if it may be technically difficult or expensive.

Non-linear optical effects have recently become fashionable and it is of some point to survey these with brief phenomenological explanations for the sake of completeness and with the intention of looking at whether instrumentation advances are likely to make them of engineering interest. Although in some cases an effect may be rather obscure, its realization may have a large impact in the real world; at least one of these effects has offered a potentially very definite way of enhancing the usefulness of the technique for

physically important measurements and that is Coherent Anti-Stokes Raman Scattering (CARS). There has appeared a plethora of acronyms and as these are becoming common in the literature we shall adhere to this usage as we have in earlier sections. There seems little point here in even discussing all the second order effects treated in Reference 4 except to give sufficient information to show why they could not be candidates for this application.

(e) Inverse Raman: This is a very weak process and its application depends on the small change in Anti-Stokes absorption of a broad band source in the presence of an intense monochromatic pump. Not only must a very small change in a large signal be measured (always bad experimental technique) but the absorption of the Anti-Stokes light must be greater than the emission derived from the pump source. There seems no suggestion of feasibility in this phenomenon.

(f) Rikes (Raman Induced Kerr Effect): Again two sources, a broad-band and a pump are necessary and induced birefringence is sought. The effect has yet to be shown in gases; even without the low concentration considerations, the technique does not merit further discussion here.

(g) Stimulated Raman: Stokes photons scattered coherently in the same direction as the laser pump experience lasing gain. The effect is only manifest in certain gases and for certain transitions, none of which is available here.

(h) Hyper Raman: This corresponds to the second harmonic term of the usual Raman process and is vestigially weak even at very high molecular densities.

(i) HORSES (Higher Order Raman Spectral Excitation): These correspond to multiphoton processes and second order effects of these. They were observed during experiments in CARS which is rather better studied and described. It offers much less feasibility than CARS.

(j) CARS (Coherent Anti-Stokes Raman Scattering): This again is a four wave parametric process requiring two incident laser beams. The difference in frequency between them must correspond to a vibrational or electronic resonance of the molecule in question and they must be phase coherent and diffraction limited over the sampling region. The pump beam, frequency ω_1, is inelastically scattered from the Stokes level excited by ω_2, ($\omega_1 > \omega_2$) and the emission frequency is $2\omega_1 - \omega_2$ which is toward the Anti-Stokes side of the vibration transition. The resultant line emission is coherent with the original beams making the collection of all the scattered light easy and because it is on the higher energy side of the system it is much more readily resolved from noise and parasitic effects such as laser induced fluorescence in other species. This is a technique for which there is much enthusiasm for identification of species present at low concentration because the available enhancement from coherent emission is very considerable.[17]

One recently reported technique is worthy of consideration, perhaps because it is still sufficiently new that its disadvantages have not all been discovered yet and therefore it is deemed to offer hope.

(k) SONRES (Saturated Optical Nonresonant Emission Spectroscopy): This method could only be used for detection of trace sodium if there were some suitable method of producing free Na from its molecular bound state. The technique is not susceptible to quenching becase it relies upon an equilibrium excitation/emission state, it is not particularly dependent upon input laser power provided it is above saturation threshold. Reference 18 discusses this technique and its advantages including the very high sensitivity. Measurements in a flame atomizer have measured down to a detection limit of 10^4 Na atoms/cm^3. It is not inconceivable that this technique will be used in conjunction with a method of producing free sodium, with some subtle calibration techniques. The measurement is to excite the 589.6 nm line of Na and monitor transition to the ground state from the D_2 level, 589.0 nm. This method has significant advantages in avoidance of light scattered at the incident frequency.

An excellent review article is provided in Reference 20. Not only does it give a broad background on the techniques here outlined, it contains 846 references to more detailed literature. Reference 21 is another more general review article which contains a modest 117 references.

2.0 PHYSICS AND PHENOMENOLOGY OF POSSIBLE CANDIDATES

Many of the potentially usable physical principles have been discussed in the foregoing section. Here we have extracted from these the ones which may not be immediately rejected on grounds of proven infeasibility. At this stage the detailed calculations are not included as they will comprise the first part of Task 2.

2.1 Direct Possibles

The direct measurement of concentration of gaseous sodium sulfate would be the first preference readout. From this the condensation point may be inferred and the approach to this point used to control bed conditions or additives to maximize operating efficiency while maintaining adequate turbine life. The only candidate method which seems to offer even a suggestion of feasibility for a non-extraction system is resonant absorption. This would require line of sight access to the flue gas, non-degrading windows and rather better knowledge of the infrared spectra of constituents species than is currently available.

This technique will be studied in depth as part of Task 2 and additional data may be obtained from measurement of spectral properties not available to the resolution required in the open literature. The details of this method are extremely simple but the chance of success depends on many factors not yet available. These are (a) adequate confidence that the spectrum of sodium sulfate contains usable lines at the temperature and pressure here, (b) further data that there are no constituents present that have spectral lines which overlap the potential desired one and have concentrations which might swamp the measurement, (c) knowledge that will guarantee suitable windows that will not change their transmission characteristics, or get dirty over a long period. Given adequate answers to these questions the problems then become those associated with guaranteeing accuracy/precision in the hostile environment. These engineering problems are at least susceptible of

solution with sufficient financial resources once the physics is shown to give a good probability of success.

From current technology no other technique is seen to be applicable to the non-sampling, non-intrusive, measurement of gaseous sodium sulfate at the specified levels in the environment of efflux from an FBC. There may be future technological developments which could alter this conclusion but it is not realistic to assume that this will happen.

2.2 Indirect Possibles

The assumptions of thermochemical equilibrium are shown to hold and if sodium containing species, other than sodium sulfate, can be monitored, together with factors affecting equilibrium conditions such as pressure and temperature, then the sulfate concentration may be inferred. Other species of relevance might be sodium chloride, hydroxide or oxides and dimers of these. Each of these might also be measured by resonant absorption if suitable spectral lines are shown to exist. Figure C-7 shows somewhat low resolution spectra for the nujol mull or for the purely solid form of NaOH and NaCl. There exist lines in the NaOH spectrum but the concentration of this is not easy to relate to the Na_2SO_4 nor to separate the lines from others at that complex region. There are, however, significantly larger concentrations of both NaOH and NaCl than Na_2SO_4 at equilibrium. Measurement of NaCl by this method seems to offer no hope; the material is often used as a construction material for infrared spectrometers because of its excellent and uniform infrared transmission out to nearly 18 μm.

Since it is possible to make estimates of Na_2SO_4 from the equilibrial species it is possible to do the same for total sodium. If it were possible to heat a sample of the gas to cause local dissociation and ionization it may then be possible to observe sodium lines. The most prominent and easily resolved are the D lines corresponding to the electronic transitions $3^2P_{3/2} \rightarrow 3^2S_{1/2}$ and $3^2P_{1/2} \rightarrow 3^2S_{1/2}$ with yellow wavelengths of 589.0 nm and 589.6 nm respectively. Once there is free sodium it is possible to measure its quantity to very low levels — a few atoms. The problem is that the method used to produce dissociation of the strongly bound molecules will wreak such havoc in the gas that the method may be difficult to execute. It is nevertheless considered possible that a system for producing local "instantaneous" heating, *e.g.*, a pulsed laser, may make this type of observation feasible. Calculations to test this idea will be performed as part of Task 2.

Another method of producing free sodium is somewhat more obscure in that the use of this observation to infer Na_2SO_4 concentration is becoming still less direct. However it does offer many advantages. It is known that if alkali halides are fragmented by photolytic radiation of appropriate wavelength then subject to the usual momentum conservation rules a molecule may be dissociated into an unexcited halogen atom and an alkali excited into the P level. The subsequent radiation of the return to ground state identifies the alkali metal. The possibility of performing this photolytic dissociation has recently been extended to molecules as stable as NaCl by the invention of eximer lasers. In this case the most suitable wavelength would be 193 nm, that that of argon fluoride which is just sufficient to dissociate NaCl and excite the sodium. The questions to be asked of the feasibility of this are

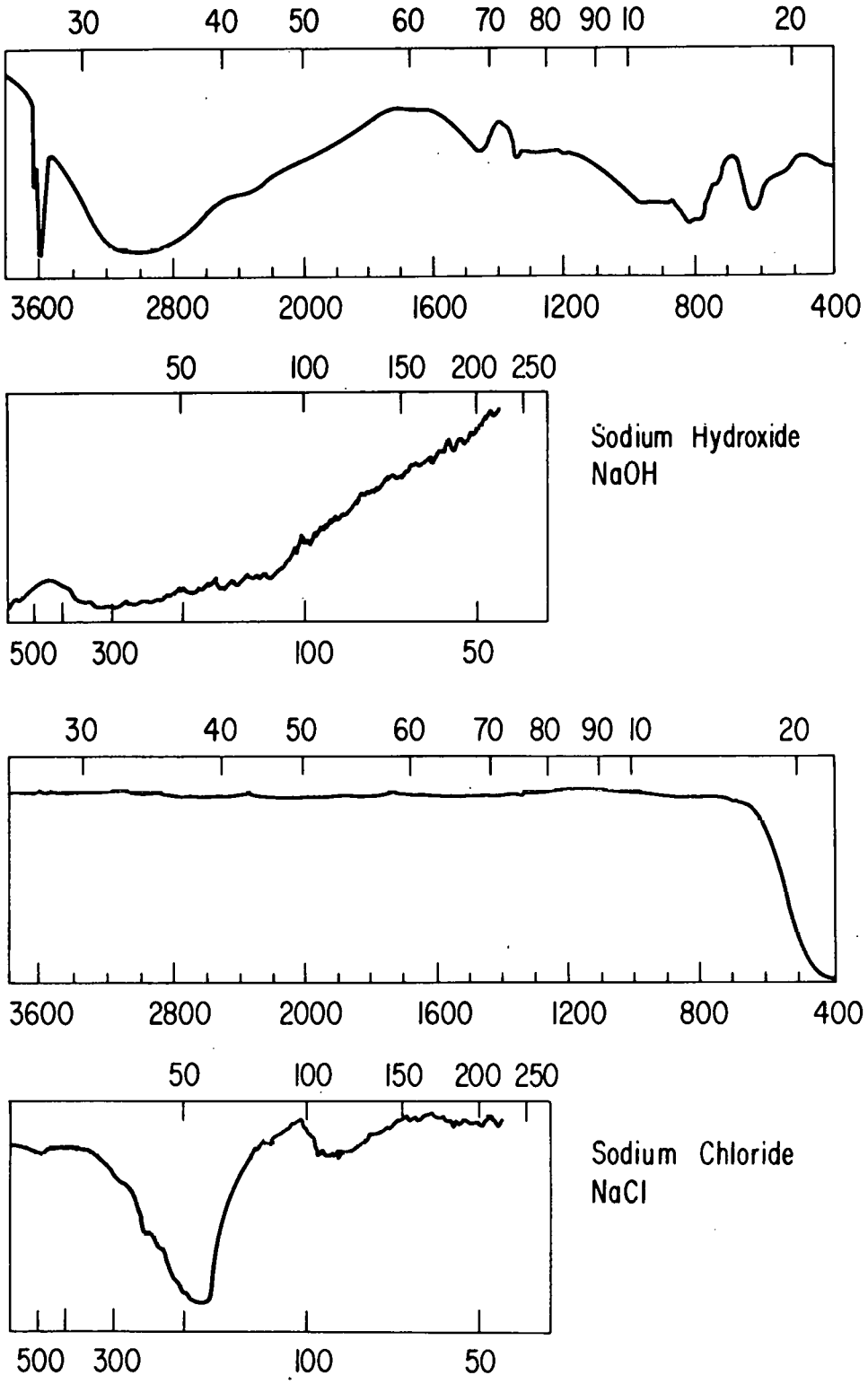

Fig. C-7. Absorption Spectra

Reproduced by permission of Academic Press. From R. Nyquist and R. O. Kagel, Infrared Spectra of Inorganic Compounds, 1971.

associated with quenching and absorption cross sections, and again a detailed analysis of this potential method is to be presented in Task 2.

2.3 Parasitic Effects

These are the effects of elastic scattering which should be considered because residual small particles in the facility may contribute to both scattering (albeit at the exciting wavelength) and absorption. The latter will probably be very small but may cause fluctuation. The inclusion of this section is not wholly redundant as there are situations where the material of which the particles are composed may be of interest. We see no reliable way of measuring the spectral distribution of scattered white light, which could in principle give some idea of the composition, at the sizes and concentrations which we are likely to obtain in this very hostile environment.

Reference 22 shows that there may be techniques capable of analyzing the constitution of small particles for many types of substance. Unfortunately that reference does not discuss sodium sulfate but has interesting and promising implications.

2.3.1 Elastic Scattering

It is thought useful and relevant to discuss elastic scattering phenomena at least in outline, not so much for completeness although this is desirable in a report such as this, but more because of the parasitic effects which may be manifested by small particles entrained in the test gases. The radiation scattered from these may in some cases make resolution of the desired radiation somewhat more difficult.

(a) Thomson: Optical photons are scattered by electrons which are either free or bound in high excited levels such that their energy of association with the atom is small compared with that of the incident photon. The cross sections for this process are exceedingly small in the optical region. Even in low angle x-ray scattering measurements of electron density in plasmas the phenomenon is not easy to translate into a measurement tool. In the high pressure high temperature case here the scattered light is of so low an intensity compared with that from the next two processes that even its potential for realizing high frequency shifts in low density electron gases may not be exploited. There seems no way to extract species type and concentration from this technique, and certainly not under these conditions.

(b) Rayleigh: Light scattered by particles small with respect to the wavelength is well understood. The light is scattered isotropically in a plane normal to the electric vector with cosine squared reduction at right-angles. Without particle motion polarization is preserved. Normally molecules fulfill this criterion and act essentially like dipoles, whose polarizability while not independent of species is by no means sufficiently strongly proportional to permit identification even of majority constituents. At ambient pressures or higher the Rayleigh scattering effect is enhanced by local density changes and multiple scattering by regions of space whose molecular density fluctuations have typical coherence lengths which still

satisfy the property of small scatterers compared with wavelength. The scattering cross section depends on λ^{-4} to first order and the consequences of this class of phenomena may be verified by observing that a clear sky is blue, the scattering being entirely dominated by submicron entropy fluctuations. Verification of the preservation of polarization is obtained by viewing the sky at dusk or dawn through Polaroid.[14] It is clear from the foregoing digression that the scattering is not sufficiently dependent on detailed molecular construction to permit its use as a trace species diagnostic technique.

(c) Mie: As the particles have a dimension of the order of the incident radiation the scattering properties become very complex, depending strongly on size referred to incident wavelength, complex refractive index, shape, etc. The basic rules for computing the scattering properties are to use Electromagnetic Field equations whose boundary conditions are satisfied at the surface of the particle. This, of course, includes reflection, refraction and diffraction. In the extreme classical case the last of these may be ignored and the first two computed from geometrical optics. For a purely reflective large sphere the light is scattered isotropically. In this case of hot high pressure gases we obviously cannot use Mie scattering to obtain details of chemical constituents of gases and probably not even of the material of which particles are made. However because there will be residual particles within the gas stream/test space it is important to quantify the effect of Mie scattering as a potential source of unwanted optical power which could mask any more appropriate measurement.

Not only do the above phenomena produce an amount of scattering proportional to their physical cross sectional area, but as the size reduces compared with the wavelength the efficienty of scattering reduces very rapidly leading to a very strong dependence of total scattered light on equivalent size. For example, if α is defined as the scattering parameter $2\pi a/\lambda$, where a is the particle radius and λ is the incident wavelength, then the scattering efficiency for reflecting spheres goes from 5×10^{-3} at $\alpha = 0.2$ to about 2.0 for $\alpha > 1$ with some small oscillation above $\alpha > 1$.[13]

Elastic processes involve no wavelength shift but there may be substances within the particles which will fluoresce and produce a quasi-continuum of scattered light at longer wavelengths from the exiting line. This behavior is especially likely if there are residuals of pyrolyzed hyrocarbons absorbed into more inert particles. Although from efficiency consideration there will be relatively little unoxidized organics remaining, the light levels which we may require to measure are very low and may suffer from this source of interference.

3.0 SELECTION FOR FURTHER ANALYSIS

It is, then, possible to give a "short" list of techniques which merit detailed consideration as ways of solving the measurement problem posed by this contract. Both direct and indirect are considered.

(1) Resonant Absorption of Na_2SO_4 ~ 9 μm.

(2) Thermal Ionization and Assay of Total Sodium.

(3) Photolytic Dissociation of NaCl and Assay of Sodium.

These three techniques are considered the most likely approaches given the existing constraints. They will be considered in much greater depth as a part of Task 2 and promising areas will be further evaluated and if appropriate, carried through a design phase.

4.0 CONCLUSIONS

(a) Most ways of detecting trace species concentration are not usable for this application because of the hostile conditions, the very low levels and the requirement not to extract a sample.

(b) Three direct and indirect methods may offer a chance of sucessful application. These are resonant absorption near 9 μm, intense local heating to yield ionized sodium and photolytic dissociation of sodium chloride.

(c) These potential methods require detailed theoretical analysis and some additional experimental data before a selection may be made between them, or indeed in favor of any.

5.0 REFERENCES

1. Stringer, J., "High Temperature Corrosion in Aerospace Alloys," AGARD AG200.

2. Stringer, J. (Private Communication).

3. Combustion Power Company, Inc., 1346 Willow Road Menlo Park, CA 94025, "Energy Conversion from Coal Utilizing CPU-400 Technology," FE/1536-1 Final Report, Vol. I, prepared for USERDA under Contract EX-76-C-01-1536, March 1977.

4. Proceeding of the Fluidized Bed Combustion Technology Exchange Workshop, April 13-15, 1977, Vols. 1 and 2, USERDA CONF-77-447-P-1/2.

5. Kohl, F. J., Stearns, C. A., Fryberg, G. C., "Sodium Sulfate: Vaporization Thermodynamics and Role in Corrosive Flames," Metal-Slag-Gas Reactions and Processes, Ed. Z. A. Foroulis and W. W. Smeltzer, The Electrochemical Society, 1975.

6. Solar Division of International Harvester, "An Investigation of Hot Corrosion and Erosion Occurring in a Fluid Bed Combustor-Gas Turbine Cycle Using Coal as Fuel," FE/1536-2, prepared for USERDA, May 1977.

7. Spectron Development Laboratories, Inc., "Laser Interferometer Analysis of Flue Gas Particles from a Fluidized Bed Combustor," FE/2413-1, prepared for USERDA under Contract EX-76-C-01-2413, April 1977.

8. Stearns, C. A., Miller, R. A., Kohl, Fred J., Fryburg, G. C., "Gaseous Sodium Sulfate Formation in Flames and Flowing Gas Environment," NASA TM X-73600, 1977.

9. Fryburg, G. C., Miller, R. A., Stearns, C. A., Kohl, F. J., "Formation of Na_2SO_4 and K_2SO_4 in Flames Doped with Sulfur and Alkali Chlorides and Carbonates," NASA TM 73794, 1977.

10. Marcote, R. V., "Fossil-Fuel Power Generation and Emissions Monitoring Requirements," ISA IPI 75459 (41-48), 1975.

11. Phillips, K. E., "Granular Bed Filter Development Program," FE/2579-3, Combustion Power Company, Inc., 1346 Willow Road, Menlo Park, CA 94025, July 1977, USERDA Contract No. EF-77-C-01-2579.

12. Appendix 'B', ANL Source Document, Contract No. 31-109-38-4107.

13. Kerker, M., The Scattering of Light, Academic Press (1969).

14. Minnaert, M., Light and Colour in the Open Air, Dover (1959).

15. Lapp, M., Penney, C., Laser Raman Gas Diagnostics, Plenum (1974).

(contd)

16. Eckbreth, A. C., Bonczyk, P. A., Verdieck, J. F., Review of Laser Raman and Fluorescence Techniques for Practical Combustion Diagnostics, UTRC R77-952665-6, EPA Contract 68-02-2176.

17. Pealat, M., Raman Spectroscopy in Flames and Reactive Media-Proceedings of the Laser Methods in Combustion Workshop, Urbino, 7-9 September 1977, Italy.

18. Gelbwachs, J. A., Klein, C. F., Wessel, J. E., "Single Atom Detection by SONRES," IEEE Journal of Quantum Electronics, Vol. QE-14, No. 2, February 1978.

19. Ximer Laser Special Issue, January 1979, IEEE Journal of Quantum Electronics (to be published).

20. Kimel, S., and Speiser, S., "Lasers and Chemistry", Vol. 77, No. 4, August 1977, pp. 437-472.

21. Self, S. A., and Kruger, G. H., "Diagnostics Methods in Combustion MHD Flows," AIAA Journal of Energy, Vol. 1, No. 1, January-February 1977, pp. 25-43.

22. Wright, M. L., "Feasibility Study of In Situ Source Monitoring of Particulate Composition by Raman and Fluorescence Scatter," EPA-R2-73-219, June 1973.

Distribution of ANL/CEN/FE-78-4

Internal:

L. Burris
W. L. Buck
F. Cafasso
E. Carls
P. T. Cunningham
J. Fischer
H. Huang
B. R. Hubble
I. Johnson (20)
A. A. Jonke (30)
J. A. Kyger
R. V. Laney
S. Lawroski
S. H. Lee
J. F. Lenc
W. A. Ellingson
L. Cuba
G. M. Kesser
E. G. Pewitt
F. F. Nunes
W. Podolski
J. Royal
S. Siegel
J. W. Simmons
G. W. Smith
R. B. Snyder
W. M. Swift
F. G. Teats
S. Vogler
E. M. Bohn
R. G. Matlock
D. S. Moulton
D. S. Webster
W. I. Wilson
J. Young
R. Bane
E. J. Croke
J. D. Gabor
K. Jensen
N. Sather
J. Shearer
E. Smyk
C. B. Turner
A. B. Krisciunas
ANL Contract File
ANL Libraries (5)
TIS Files (6)

External:

DOE-TIC, for distribution per UC-90e (256)
Manager, Chicago Operations Office
Chief, Office of Patent Counsel, CH
V. H. Hummel, Chicago Operations Office
President, Argonne Universities Association
Chemical Engineering Division Review Committee:
- C. B. Alcock, U. Toronto
- R. C. Axtmann, Princeton Univ.
- R. E. Balzhiser, Electric Power Research Institute
- J. T. Banchero, Univ. Notre Dame
- T. Cole, Ford Motor Co.
- P. W. Gilles, Univ. Kansas
- R. I. Newman, Allied Chemical Corp.
- G. M. Rosenblatt, Pennsylvania State Univ.

S. Saxena, Univ. Illinois, Chicago
D. H. Archer, Westinghouse Research Labs.
E. C. Bailey, John Dolio and Associates
S. Beall, Oak Ridge National Laboratory
O. L. Bennett, West Virginia U.
R. Bertrand, Exxon Research and Engineering (5)
M. Boyle, Valley Forge Labs.
J. A. Brooks, Amoco Oil Co.
R. D. Brooks, General Electric Co.
C. Busch, Spectron Development Laboratory, Inc.
J. Chen, Lehigh U.
D. Cherrington, Exxon Research and Engineering Co., Florham Park, NJ
J. Clark, Tennessee Valley Authority
D. Clarke, Stearns-Rogers
N. Coates, The MITRE Corporation
R. C. Corey, DOE-CCU
R. Covell, Combustion Engineering, Inc.

G. Curran, Conoco Coal Development Co.
D. DeCoursin, Fluidyne Engineering Co.
J. Dodge, Tetra Tech, Inc.
T. E. Dowdy, Babcock and Wilcox Company
M. Dudukovic, Washington U.
S. Ehrlich, Electric Power Research Institute
M. Evans, Aerotherm Division of ACUREX Corporation
M. H. Farmer, Exxon Research & Engineering Co., Linden, NJ
C. Fisher, Univ. Tennessee
T. Fitzgerald, Oregon State U.
J. F. Flagg, Universal Oil Products Co.
H. B. Forbes, Stone & Webster Engineering Corp.
V. Forlenca, Englehard Industries
R. L. Gamble, Foster Wheeler Energy Corporation
D. E. Garrett, Garrett Energy Research and Engineering, Inc.
L. Gasner, U. Maryland
J. Geffken, DOE-CCU (5)
C. Georgakis, Massachusetts Inst. Technology
R. Glenn, Combustion Processes, Inc.
J. S. Gordon, TRW, Inc., McLean, VA
O. J. Hahn, Univ. Kentucky
W. Hansen, Babcock & Wilcox Co., Barberton, O.
M. J. Hargrove, Combustion Engineering, Inc.
R. D. Harvey, Illinois State Geological Survey
R. Helfenstein, Illinois State Geological Survey
R. G. Hickman, Lawrence Livermore Lab.
D. Huber, Burns & Roe, Inc., Paramus, NJ
F. D. Hutchinson, Gibbs and Hill
D. L. Keairns, Westinghouse Research Laboratories
W. E. Kramer, Fluidized Combustion Co.
H. Lange, Babcock & Wilcox Co., Alliance, O.
C. B. Leffert, Wayne State University
A. M. Leon, Dorr-Oliver, Inc.
R. M. Lundberg, Commonwealth Edison Co.
J. J. Markowsky, American Electric Power Service Corp., New York City
W. McCurdy, DOE-CCU
J. Mesko, Pope, Evans and Robbins (2)
T. A. Milne, Solar Energy Research Institute
W. G. Moore, Dow Chemical, USA
S. Moskowitz, Curtiss-Wright Corporation
W. Norcross, Combustion Engineering, Inc.
T. A. Pearce, Dow Chemical
W. A. Peters, Massachusetts Institute of Technology
C. Petty, Michigan State U.
R. Reed, Pope, Evans and Robbins, Inc.
J. T. Reese, Tennessee Valley Authority
A. F. Sarofim, Massachusetts Institute of Technology
R. D. Smith, Combustion Power Company, Inc.
C. Space, Reynolds, Smith & Hills, Jacksonville, FL
W. K. Stair, Univ. Tennessee
F. Staub, General Electric Corp., Schenectady
W. Steen, U. S. Environmental Protection Agency (16)
M. Steinberg, Brookhaven National Laboratory
W. Strieder, Univ. Notre Dame

S. E. Tung, Massachusetts Institute of Technology
V. Underkoffler, Gilbert Associates, Inc.
F. A. Walton, Combustion Power Co.
A. E. Weller, Battelle Columbus Labs.
T. D. Wheelock, Iowa State University
J. S. Wilson, Morgantown Energy Research Center
K. Yeager, Electric Power Research Inst.
D. Zallen, Energy and Environmental Research Corp., Santa Ana
R. E. Zoellner, Stearns-Roger
J. Highley, U.K. National Coal Board, England
H. R. Hoy, BCURA Ltd., England
H. Schreckenberg, Bergbau-Forschung GmbH, Germany
G. Moss, Esso Research Centre, England
B. A. Wiechula, Imperial Oil Enterprises, Canada

U.S. GOVERNMENT PRINTING OFFICE: 1978—650-326